Doctoral Thesis

Assessing Sediment Yield in Steep Mountainous Catchment: Influences, Management, and High Temporal Modeling under Various Land Use and Soil Types

September 2024

Nang Yu War

Graduate School of Advanced Science and Engineering

Hiroshima University

Abstract

Rainfall-induced floods and suspended sediments impact both water quality and human well-being. Besides the impact of soil erosion on the environment, the soil itself is a very fragile and valuable resource due to the difference between soil formation and deterioration rates. Japanese catchments are vulnerable to flood and sediment-related disasters as steep slope catchments are under torrential rainfall despite forests being the dominant land use types. This study utilized the Soil and Water Assessment Tool (SWAT) and assessed the high-sediment-yield areas, identified the main factors for high sediment yield, evaluated the effectiveness of filter strips in retaining the sediment from steep slope areas, and analyzed the pre-event and within-event conditions on the simulation of the sub-daily hydrological model. The model results showed that SWAT is a reliable model to simulate sediment transport successfully pointing out the high sediment yield hotspot areas. The slope is the most influencing factor for the high sediment and consequently, steep slopes along the river are the most critical areas for sediment production. The slope gradient effects are varied with different land use and soil types. Deciduous forests with a slope gradient greater than 45% rise are the areas with the highest soil erosion rate. Regosol soil types showed the highest soil erosion rate as the slope became steeper. The sediment filter

strips revealed to be effective for trapping the sediments transported from the steep slope, with the 5-m width strip in the five highest sediment yield subbasins retaining 14% of the total sediment transported at the catchment main outlet. Additionally, the SWAT model can satisfactorily simulate high-flow events despite the model performance being related to the event conditions and characteristics. Moist antecedent conditions with low total precipitation events' streamflow and suspended sediment are simulated satisfactorily by the sub-daily model. The sub-daily event-based model provides better simulation than the time-continuous daily model in high-flow events simulation. The transported sediment during the high-flow events is influenced not only by the total precipitation of the event but also by the spatial variation of precipitation in the catchment, where the concentrated precipitation in high sediment yield subbasin events transported a higher amount of sediment than the other events. Therefore, future studies focusing on the spatial precipitation input data on the sub-daily model simulation are preferable. As the steep slope is the highest influencing factor on sediment yield, the influence of the topography input data resolution on the catchment sediment simulation should be addressed in the future.

Acknowledgements

First and foremost, I would like to express my sincere gratitude to my supervisor, Dr. Shin-ichi Onodera. Your unwavering support, insightful guidance, and constant encouragement have been invaluable throughout this research. I am grateful for the opportunity to carry out this work under your supervision, and I appreciate the time and effort you have dedicated to helping me throughout this journey.

I am deeply grateful to the members of my thesis committee, Dr. Hisashi Ozawa, Dr. Tadashi Yokoyama, Dr. Han Soo Lee, Dr. Yoko Iwamoto, and Dr. Mitsuyo Saito for their insightful feedback and valuable suggestions, which have greatly enhanced my research.

I would like to extend my sincere thanks to my seniors and friends at Hiroshima University. Your support and camaraderie have been invaluable throughout this journey. I am especially grateful to Dr. Yuta Shimizu, Dr. Kunyang Wang and Dr. Sharon Bih Kimbi for their crucial suggestions and for always being there to lend a helping hand.

I would like to acknowledge the financial support provided by the Japan Cooperation Agency (JICA), which made it possible for me to undertake this research. Without this support, completing this thesis would not have been possible.

I am profoundly grateful to my family for their unwavering support and understanding. My greatest source of strength comes from my parents' trust in me and their constant support. My siblings, my sister-in-law, and my little niece, your love and support have been a comforting presence throughout this journey. My sincere gratitude goes to my dearest sister, my personal health caretaker, for always caring for my medical needs.

Finally, I would like to thank all those who have contributed, in various ways, to the successful completion of this thesis. Whether through academic support, emotional encouragement, or simply by being there, you have all played a part in this achievement, and for that, I am deeply grateful.

Table of contents

List of figures

List of Tables

Chapter 1 Introduction

1.1 Background

Soil is a nonrenewable resource, and the difference between the soil formation rate from natural geological processes and the possible rate of soil deterioration makes the soil a very fragile and valuable resource (Kirkby & Morgan, 1980). As the present soil erosion rates are higher in magnitude than soil formation, it has been a major threat to food security and the sustainability of ecosystems (Wuepper et al., 2019).

Soil erosion hampers the United Nation's (UN) Sustainable Development Goals (SDGs) in numerous ways. For instance, the Food and Agriculture Organization claimed that soil erosion threatens food security by hindering the production of nutritious foods, promoting ecosystem degradation, influencing water supplies, causing damage to urban infrastructure, contributing to poverty, and leading to migration. Sedimentation in reservoirs decreases their storage capacity and lowers their drinking water quality, thereby impacting clean water and sanitation. Moreover, the sediments washed away from upland areas, transported by rivers, and deposited in coastal areas, can exacerbate coral reef cover, affecting the life below water (Borrelli et al., 2020; UN General Assembly, 2015).

Climate, soil characteristics, topography, and ground cover are the principal factors affecting water erosion. Soil erosion intensity varies on the precipitation intensity, duration, total amount, and size of droplets (Gray & Leiser, 1982; Lull, 1959). Soil structure and texture, organic matter content, and permeability determine the soil erodibility (Bonilla & Johnson, 2012; Wischmeier & Mannering, 1969). A large part of the runoff velocity is determined by the slope length and steepness, thus being critical in

soil erosion potential (Liu et al., 2000). Ground cover, including natural and anthropogenic structures, influences surface runoff and erosion (İlay & Kavdir, 2018; Zhou et al., 2008).

1.1.1 Assessment of soil erosion in steep slope catchments

Forested catchments play a vital role in high-quality water supplies and provide slope stability and erosion control worldwide (Barten & Ernst, 2004; Marden, 2012; Webb et al., 2012). However, forested catchments tend to exist in regions with high precipitation, which could increase material discharge into streams (Brooks et al., 1991; Hancock et al., 2017). This is the same for Japan's steep, forested catchments with high precipitation, which transport mass sediment yield and cause flood and sediment disasters (Uchida et al., 2017; Hayashi et al., 2022). During intense rainfall, steep slope catchments with unstable soil are prone to debris flow, which can block the waterway, thereby making the urban runoff flow into the drainage channel difficult, which consequently causes flooding in the urban areas (Hua, 2024).

Soil erosion assessments are mainly carried out by either experimental measurements or erosion prediction models (Gholami et al., 2021; Ketema & Dwarakish, 2021; Salumbo, 2020; Wakiyama et al., 2010). The use of erosion models has increased over time as they can provide wide-area and long-term assessment at a low cost. Moreover, modelling can provide simulation scenarios (management scenarios, land use and climate change scenarios), which are helpful for effective watershed management (Pandey et al., 2016; Salumbo, 2020).

1.1.2 Soil conservation strategies and management practices for steep slope catchments

Soil and water quality conservation in catchments with steep slopes requires controlling soil erosion and sediment yield. Implementing efficient soil conservation and management techniques can greatly reduce erosion and improve the long-term viability of these landscapes (Mekonnen et al., 2015). One of the most effective soil conservation measures is establishing and maintaining vegetative cover, as plants and trees help stabilize the soil with their root systems, reduce the speed of surface runoff, and increase water infiltration into the soil (Morgan, 2005). On steep slopes, a combination of trees, shrubs, and grasses is frequently utilized to create a protective canopy (Montgomery, 2007). For example, in contour planting, crops are planted along the contour lines of the slope to help reduce soil erosion by slowing down water runoff (Gyssels et al., 2005).

Managing steep slope catchments requires the application of appropriate land use practices. By incorporating trees and shrubs into agricultural systems, agroforestry improves soil stability and lowers erosion (Walling, 1983). Furthermore, avoiding soil disturbance through plowing, or "no-till" farming, contributes to preserving soil structure and lowering erosion (Lal, 2001).

In addition to vegetation and land use practices, structural measures such as terracing, check dams, and retaining walls play a significant role in soil conservation (Pimentel & Kounang, 1998). Terracing can reduce the gradient and slows down water flow, thereby reducing erosion. Moreover, small barriers like check dams help in trapping sediments and reducing the velocity of water. Additionally, retaining walls provide support to the soil and prevent it from sliding down the slope (Morgan, 2005). However, these structures

need to be designed carefully according to the specific conditions of the catchment (Pimentel & Kounang, 1998). Table 1 summarizes an assessment of best management practices by different modelling approaches from previous studies.

Table 1 Summary of previous studies on the assessment of best management practices

Study area	Methodology	Management practices assessed	Main finding	References
Nashe Watershed, Ethiopia	SWAT	Filter strip, Stone/soil bunds, Contouring, terracing	Stone/soil bunds and terracing reduce the maximum sediment yield	Leta et al. (2023)
Mill River, Canada	SWAT, ANFIS	Riparian buffer strips, assess the different buffer strips width	50-m buffer width is the most effective	Sirabahenda et al. (2020)
Joumine watershed, Tunisia	SWAT	Detention/ sediment ponds, Contour ridges, Grass strip cropping, No-till farming, Buffer strips	Ponds and buffer strips are the most effective, contour ridges are effective for gentle slope	Mtibaa et al. (2018)
Big Sunflower River watershed, Mississippi river	SWAT	Vegetated filter strips, Grade stabilization structures, Grasses waterways, Combined management practices	Combined management practices are more effective than individuals	Nepal & Parajuli (2022)
Upper Gilo watershed, Ethiopia	SWAT	Filter strip, Terracing, Contouring	Contouring is the most beneficial	Zantet oybitet et al. (2023)
Experimental plot	Physically based multifaceted model	Vegetative filter strip	sediment trapping efficiency is more sensitive to slope gradient, inflow discharge, and VFS length	Wu et al. (2023)

Study area	Methodology	Management practices assessed	Main finding	References
Baitarani watershed, India	SWAT	Conservation tillage, contour farming, contour bunding, bench terracing, loose boulder check dams, grade stabilize structures, streambank stabilization structures, contour stone bunding	Structural management practices are the most effective, combined management practices decrease surface runoff and increase subsurface flow	Uniyal et al. (2020)
Experimental plot	Vegetative filter strips modeling system	Assessment of filter strip length	effective BMPs even in steep, short-slope conditions	Zhang et al. (2023)
Gojeb watershed, Ethiopia	SWAT	Reforestation of bare land, hillside terraces, grassed filter strips	Hillside terraces have the highest efficiency	Anteneh et al. (2023)
Upper Blue Nile Basin, Ethiopia	SWAT	Filter strips, stone bund, reforestation	Filter strips are the most effective	Betrie et al. (2011)
Daketa sub-basin, Ethiopia	SWAT	Filter strips, grass waterways, Terracing	Grass waterways are the most effective	Hassen et al. (2022)

Note: SWAT (Soil and Water Assessment Tool), ANFIS (Adaptive Neuro-Fuzzy Inference System), BMPs (Best Management Practices)

1.1.3 Temporal resolution in hydrological modeling

The temporal resolution in hydrological modelling is crucial for accurately capturing hydrological processes and achieving reliable simulation results (Ficchì et al., 2016). Temporal resolution refers to the time step used in the model to simulate various hydrological processes. Studies have shown that different temporal resolutions can

significantly impact the model's output and its ability to represent actual phenomena in reality (Abbaspour et al., 2015; Arnold et al., 1998; Neitsch et al., 2011).

Daily temporal resolution is commonly used in hydrological modelling, including Soil and Water Assessment Tool (SWAT), due to its balance on computational efficiency and accuracy (Gassman et al., 2007; Srinivasan & Sathiya, 2010). Daily time steps are used to capture seasonal variations and long-term trends in hydrological processes without being overly demanding in terms of data and computational resources. However, certain hydrological events, like peak runoff during intense storms, may not be well-represented at a daily resolution (Di Luzio et al., 2005; Jeong et al., 2010). In extreme runoff events, finer temporal resolutions, such as sub-daily or hourly, can capture a more detailed representation of hydrological processes, especially for the peak flows and the timing of runoff events (Tan et al., 2020). However, the increase in data requirements and the computational demands of sub-daily simulations can be a limiting factor for their widespread use (Brighenti et al., 2019).

1.2 Objectives

The main objective of this study is to assess the sediment yield variation and its influencing factors in a steep flood-vulnerable catchment.

The specific objectives are to identify high sediment yield areas, investigate the main influencing factors for high sediment yield, assess the effectiveness of filter strips in retaining sediment, and evaluate the performance of the hourly SWAT model for extreme events in relation to the pre-antecedent conditions of the events.

1.3 Flow and structure overview

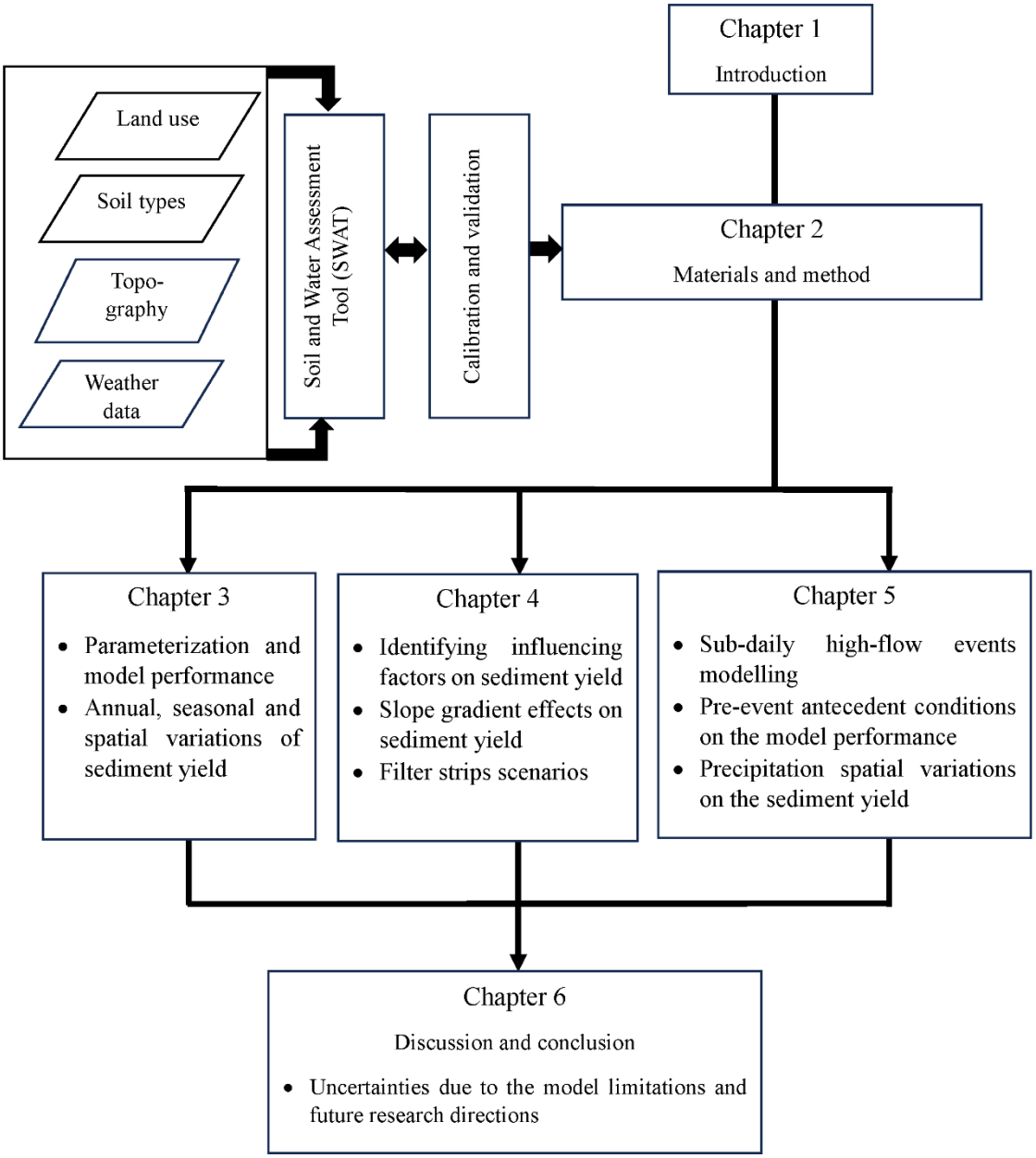

Figure 1 Flow and structure of this study

1.4. References

Abbaspour, K. C., Rouholahnejad, E., Vaghefi, S., Srinivasan, R., Yang, H., & Kløve, B. (2015). A continental-scale hydrology and water quality model for Europe: Calibration and uncertainty of a high-resolution large-scale SWAT model. Journal of Hydrology, 524, 733–752. https://doi.org/10.1016/j.jhydrol.2015.03.027

Anteneh, Y., Alamirew, T., Zeleke, G., & Kassawmar, T. (2023). Modeling runoff-sediment influx responses to alternative BMP interventions in the Gojeb watershed, Ethiopia, using the SWAT hydrological model. Environmental Science and Pollution Research, 30(9), 22816–22834. https://doi.org/10.1007/s11356-022-23711-4

Arnold, J. G., Srinivasan, R., Muttiah, R. S., & Williams, J. R. (1998). Large area hydrologic modeling and assessment part I: Model development. Journal of the American Water Resources Association, 34(1), 73–89. https://doi.org/10.1111/j.1752-1688.1998.tb05961.x

Barten, P. K., & Ernst, C. E. (2004). Land Conservation and Watershed Management for Source Protection. Journal - American Water Works Association, 96(4), 121–135. https://doi.org/10.1002/j.1551-8833.2004.tb10603.x

Betrie, G. D., Mohamed, Y. A., Van Griensven, A., & Srinivasan, R. (2011). Sediment management modelling in the Blue Nile Basin using SWAT model. Hydrology and Earth System Sciences, 15(3), 807–818. https://doi.org/10.5194/hess-15-807-2011

Bonilla, C. A., & Johnson, O. I. (2012). Soil erodibility mapping and its correlation with soil properties in Central Chile. Geoderma, 189–190, 116–123. https://doi.org/10.1016/j.geoderma.2012.05.005

Borrelli, P., Robinson, D. A., Panagos, P., Lugato, E., Yang, J. E., Alewell, C., Wuepper, D., Montanarella, L., & Ballabio, C. (2020). Land use and climate change impacts on global soil erosion by water (2015-2070). Proceedings of the National Academy of Sciences, 117(36), 21994–22001. https://doi.org/10.1073/pnas.2001403117

Brighenti, T. M., Bonumá, N. B., Srinivasan, R., & Chaffe, P. L. B. (2019). Simulating sub-daily hydrological process with SWAT: a review. Hydrological Sciences Journal, 64(12), 1415–1423. https://doi.org/10.1080/02626667.2019.1642477

Brooks, K. N., Ffolliott, P. F., Gregersen, H. M., & Thames, J. L. (1991). Hydrology and the management of watersheds. Iowa State University Press.

Di Luzio, M., Arnold, J. G., & Srinivasan, R. (2005). Effect of GIS data quality on small watershed stream flow and sediment simulations. Hydrological Processes, 19(3), 629–650. https://doi.org/10.1002/hyp.5612

Ficchì, A., Perrin, C., & Andréassian, V. (2016). Impact of temporal resolution of inputs on hydrological model performance: An analysis based on 2400 flood events. Journal of Hydrology, 538, 454–470. https://doi.org/10.1016/j.jhydrol.2016.04.016

Gassman, P. W., Reyes, M. R., Green, C. H., Arnold, J. G., & Gassman, P. W. (2007). The Soil and Water Assessment Tool: Historical Development, Applications, and Future Research Directions. Transactions of the ASABE, 50(4), 1211–1250.

Gholami, V., Sahour, H., & Hadian Amri, M. A. (2021). Soil erosion modeling using erosion pins and artificial neural networks. Catena, 196, 104902. https://doi.org/10.1016/j.catena.2020.104902

Gray, D. H., & Leiser, A. (1982). Biotechnical Slope Protection and Erosion Control. Van Nostrand Reinhold.

Gyssels, G., Poesen, J., Bochet, E., & Li, Y. (2005). Impact of plant roots on the resistance of soils to erosion by water: a review. Progress in Physical Geography: Earth and Environment, 29(2), 189–217. https://doi.org/10.1191/0309133305pp443ra

Hancock, G. R., Hugo, J., Webb, A. A., & Turner, L. (2017). Sediment transport in steep forested catchments – An assessment of scale and disturbance. Journal of Hydrology, 547, 613–622. https://doi.org/10.1016/j.jhydrol.2017.02.022

Hassen, S. M., Gebremariam, B., & Tenagashaw, D. Y. (2022). Sediment Yield Modeling and Evaluation of Best Management Practices Using the SWAT Model of the Daketa Watershed, Ethiopia. Water Conservation Science and Engineering, 7(3), 283–292. https://doi.org/10.1007/s41101-022-00142-3

Hayashi, S. I., Kunitomo, M., Mikami, K., & Suzuki, K. (2022). Recent and Historical Background and Current Challenges for Sediment Disaster Measures against Climate Change in Japan. In Water (Vol. 14, Issue 15). MDPI. https://doi.org/10.3390/w14152285

Hua, W. (2024). Development of numerical technique and field application using integrated simulation of river flooding and inundation for disaster prevention and mitigation. Okayama University.

İlay, R., & Kavdir, Y. (2018). Impact of land cover types on soil aggregate stability and erodibility. Environmental Monitoring and Assessment, 190(9), 525. https://doi.org/10.1007/s10661-018-6847-4

Jeong, J., Kannan, N., Arnold, J., Glick, R., Gosselink, L., & Srinivasan, R. (2010). Development and Integration of Sub-hourly Rainfall-Runoff Modeling Capability Within a Watershed Model. Water Resources Management, 24(15), 4505–4527. https://doi.org/10.1007/s11269-010-9670-4

Ketema, A., & Dwarakish, G. S. (2021). Water erosion assessment methods: a review. ISH Journal of Hydraulic Engineering, 27(4), 434–441. https://doi.org/10.1080/09715010.2019.1567398

Kirkby, M. J., & Morgan, R. P. C. (1980). Soil erosion. Chichester; New York. Wiley.

Lal, R. (2001). Soil degradation by erosion. Land Degradation & Development, 12(6), 519–539. https://doi.org/10.1002/ldr.472

Leta, M. K., Waseem, M., Rehman, K., & Tränckner, J. (2023). Sediment yield estimation and evaluating the best management practices in Nashe watershed, Blue Nile Basin, Ethiopia. Environmental Monitoring and Assessment, 195(6), 716. https://doi.org/10.1007/s10661-023-11337-z

Liu, B. Y., Nearing, M. A., Shi, P. J., & Jia, Z. W. (2000). Slope Length Effects on Soil Loss for Steep Slopes. Soil Science Society of America Journal, 64(5), 1759–1763. https://doi.org/10.2136/sssaj2000.6451759x

Lull, H. W. (1959). Soil Compaction on Forest and Range Land. Forest Service, U.S. Department of Agriculture.

Marden, M. (2012). Effectiveness of reforestation in erosion mitigation and implications for future sediment yields, East Coast catchments, New Zealand: A review. New Zealand Geographer, 68(1), 24–35. https://doi.org/10.1111/j.1745-7939.2012.01218.x

Mekonnen, M., Keesstra, S. D., Stroosnijder, L., Baartman, J. E. M., & Maroulis, J. (2015). Soil Conservation Through Sediment Trapping: A Review. Land Degradation & Development, 26(6), 544–556. https://doi.org/10.1002/ldr.2308

Montgomery, D. R. (2007). Soil erosion and agricultural sustainability. Proceedings of the National Academy of Sciences, 104(33), 13268–13272. https://doi.org/10.1073/pnas.0611508104

Morgan, R. P. C. (2005). Soil Erosion and Conservation. European Journal of Soil Science, 56(5), 686–686. https://doi.org/10.1111/j.1365-2389.2005.0756f.x

Mtibaa, S., Hotta, N., & Irie, M. (2018). Analysis of the efficacy and cost-effectiveness of best management practices for controlling sediment yield: A case study of the Joumine watershed, Tunisia. Science of The Total Environment, 616–617, 1–16. https://doi.org/10.1016/j.scitotenv.2017.10.290

Neitsch, S. L., Arnold, J. G., Kiniry, J. R., & Williams, J. R. (2011). Soil and Water Assessment Tool Theoretical Documentation Version 2009.

Nepal, D., & Parajuli, P. B. (2022). Assessment of Best Management Practices on Hydrology and Sediment Yield at Watershed Scale in Mississippi Using SWAT. Agriculture, 12(4). https://doi.org/10.3390/agriculture12040518

Pandey, A., Himanshu, S. K., Mishra, S. K., & Singh, V. P. (2016). Physically based soil erosion and sediment yield models revisited. Catena (Vol. 147, pp. 595–620). Elsevier B.V. https://doi.org/10.1016/j.catena.2016.08.002

Pimentel, D., & Kounang, N. (1998). Ecology of Soil Erosion in Ecosystems. Ecosystems, 1(5), 416–426. https://doi.org/10.1007/s100219900035

Salumbo, A. M. de O. (2020). A Review of Soil Erosion Estimation Methods. Agricultural Sciences, 11(08), 667–691. https://doi.org/10.4236/as.2020.118043

Sirabahenda, Z., St-Hilaire, A., Courtenay, S. C., & van den Heuvel, M. R. (2020). Assessment of the effective width of riparian buffer strips to reduce suspended sediment in an agricultural landscape using ANFIS and SWAT models. Catena, 195, 104762. https://doi.org/10.1016/j.catena.2020.104762

Srinivasan, R., & Sathiya, K. (2010). Experimental study on Bagasse Ash in concrete. International Journal for Service Learning in Engineering, Humanitarian Engineering and Social Entrepreneurship, 5(2), 60–66. https://doi.org/10.24908/ijsle.v5i2.2992

Tan, M. L., Gassman, P. W., Yang, X., & Haywood, J. (2020). A review of SWAT applications, performance and future needs for simulation of hydro-climatic extremes. In Advances in Water Resources (Vol. 143). Elsevier Ltd. https://doi.org/10.1016/j.advwatres.2020.103662

Uchida, T., Sakurai, W., & Okamoto, A. (2017). Historical Patterns of Heavy Rainfall Event and Deep-Seated Rapid Landslide Occurrence in Japan: Insight for Effects of Climate Change on Landslide Occurrence. In Advancing Culture of Living with Landslides, 251–257.

UN General Assembly. (2015, October 21). Transforming our world: the 2030 Agenda for Sustainable Development.

Uniyal, B., Jha, M. K., Verma, A. K., & Anebagilu, P. K. (2020). Identification of critical areas and evaluation of best management practices using SWAT for sustainable watershed management. Science of the Total Environment, 744. https://doi.org/10.1016/j.scitotenv.2020.140737

Wakiyama, Y., Onda, Y., Mizugaki, S., Asai, H., & Hiramatsu, S. (2010). Soil erosion rates on forested mountain hillslopes estimated using 137Cs and 210Pbex. Geoderma, 159(1–2), 39–52. https://doi.org/10.1016/j.geoderma.2010.06.012

Walling, D. E. (1983). The sediment delivery problem. Journal of Hydrology, 65(1–3), 209–237. https://doi.org/10.1016/0022-1694(83)90217-2

Webb, A. A., Dragovich, D., & Jamshidi, R. (2012). Temporary increases in suspended sediment yields following selective eucalypt forest harvesting. Forest Ecology and Management, 283, 96–105. https://doi.org/10.1016/j.foreco.2012.07.017

Wischmeier, W. H., & Mannering, J. V. (1969). Relation of Soil Properties to its Erodibility. Soil Science Society of America Journal, 33(1), 131–137. https://doi.org/10.2136/sssaj1969.03615995003300010035x

Wuepper, D., Borrelli, P., & Finger, R. (2019). Countries and the global rate of soil erosion. Nature Sustainability, 3(1), 51–55. https://doi.org/10.1038/s41893-019-0438-4

Wu, S., Chui, T. F. M., Chen, L., & Chow, C. H. C. (2023). Modelling sediment trapping in vegetative filter strips on steep slopes. Hydrological Processes, 37(1). https://doi.org/10.1002/hyp.14793

Zantet oybitet, M., Sambeto Bibi, T., & Abdulkerim Adem, E. (2023). Evaluation of best management practices to reduce sediment yield in the upper Gilo watershed, Baro akobo basin, Ethiopia using SWAT. Heliyon, 9(10), e20326. https://doi.org/10.1016/j.heliyon.2023.e20326

Zhang, Y., Bhattarai, R., & Muñoz-Carpena, R. (2023). Effectiveness of vegetative filter strips for sediment control from steep construction landscapes. Catena, 226. https://doi.org/10.1016/j.catena.2023.107057

Zhou, P., Luukkanen, O., Tokola, T., & Nieminen, J. (2008). Effect of vegetation cover on soil erosion in a mountainous watershed. Catena, 75(3), 319–325. https://doi.org/10.1016/j.catena.2008.07.010

Chapter 2 Materials and method

2.1 Study area

The Takahashi River catchment, with an area of 2670 km², is located in the Okayama Prefecture of western Japan (Figure 2). The main river's total length is 111 km. The major tributaries of the Takahashi River are the Takahashi, Nariwa, and Oda Rivers. The catchment elevation ranges from 0 to 1264 m above sea level. Takahashi River originates from the forested steep slopes of mountainous areas and finally enters the Seto inland sea at Kurashiki City.

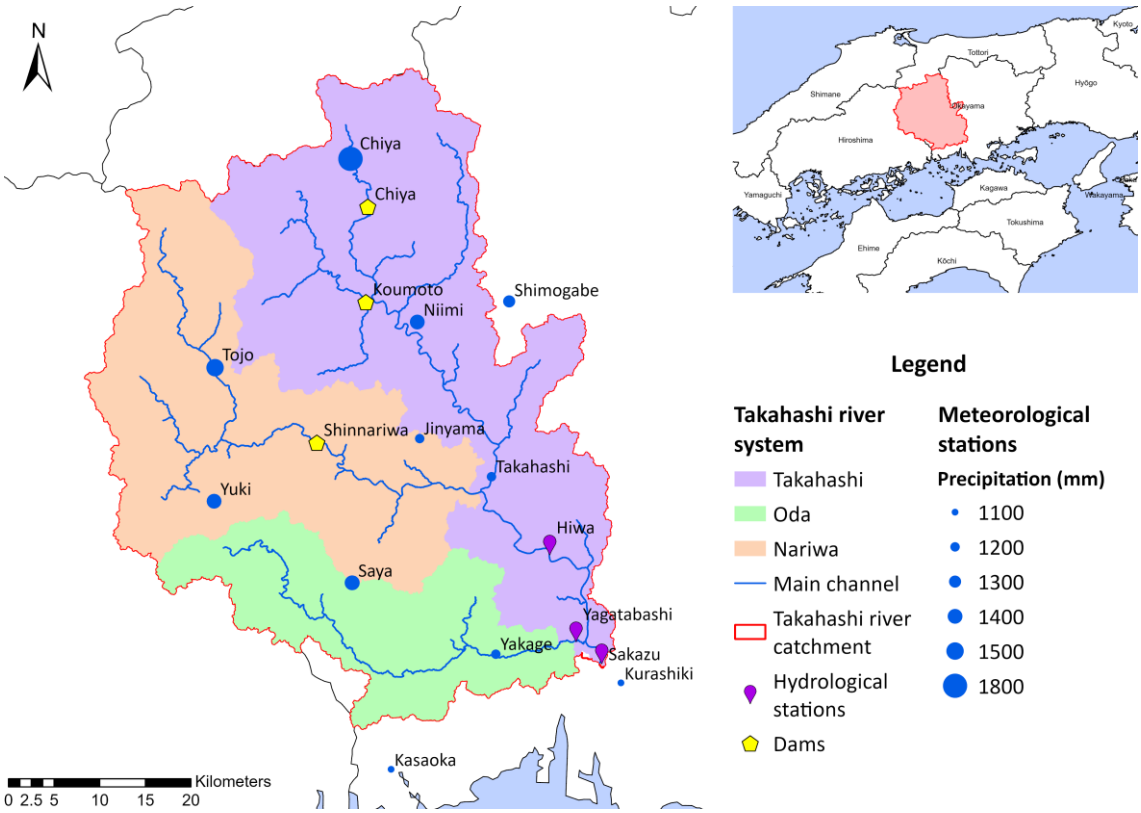

Figure 2 Takahashi river system (main tributaries, hydrological stations, dams, and meteorological stations)

The Takahashi catchment is a forested catchment with 84% forest cover, with deciduous forests at 43.74 % and evergreen at 41.05% (Figure 3). As the hydrological processes of different types of forests differ significantly, the study area had to be divided according to land use in various modelling works (Wang K. et al., 2022). The catchment mean slope is 30% and is characterized by a steep slope greater than 15%, occupying 79.15% of the catchment area (Figure 4). The dominant soil type is cambisols, representing 67.25 % of the catchment area (Figure 5). The other soil types are regosols (12.06%), andosols (10.52%), and gleysols (8.83%). The andosols and most cambisols soil areas are found in the Takahashi and Nariwa tributaries, whereas the Oda tributary mainly comprises gleysols and regosols. The mean annual precipitation across the catchment from 1990 to 2022 is 1328 mm. Takahashi catchment is undergoing increasing precipitation due to climate change, according to historical precipitation data (Figure 6).

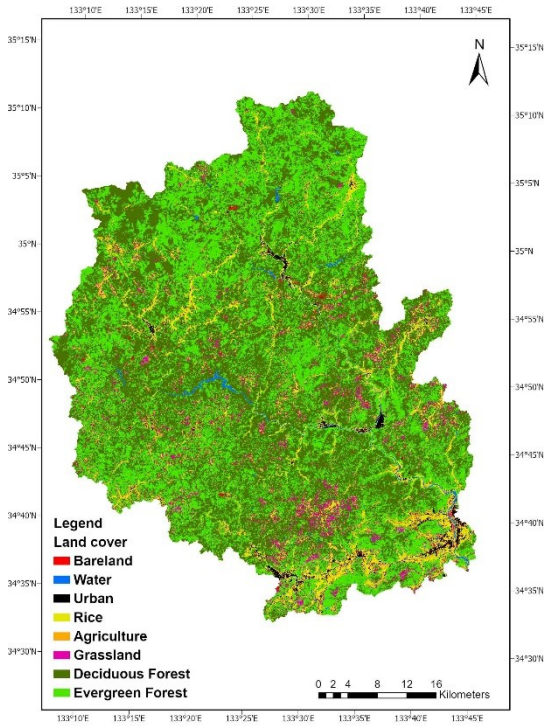

Figure 3 Land use of Takahashi catchment

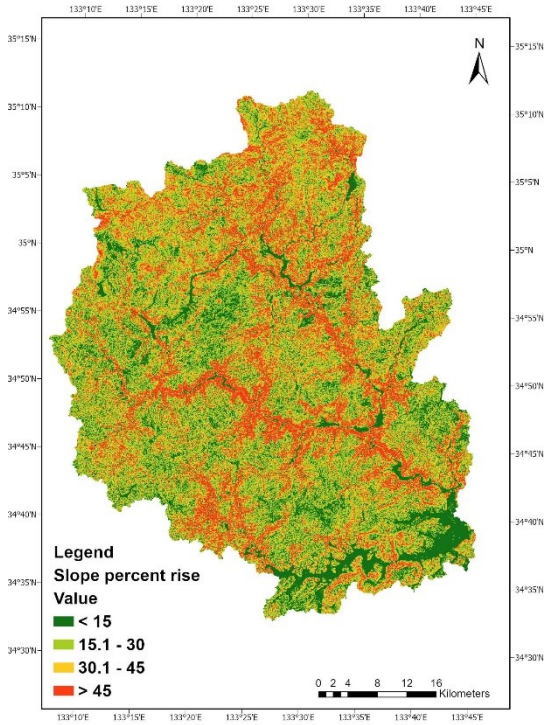

Figure 4 Slope gradient of Takahashi catchment

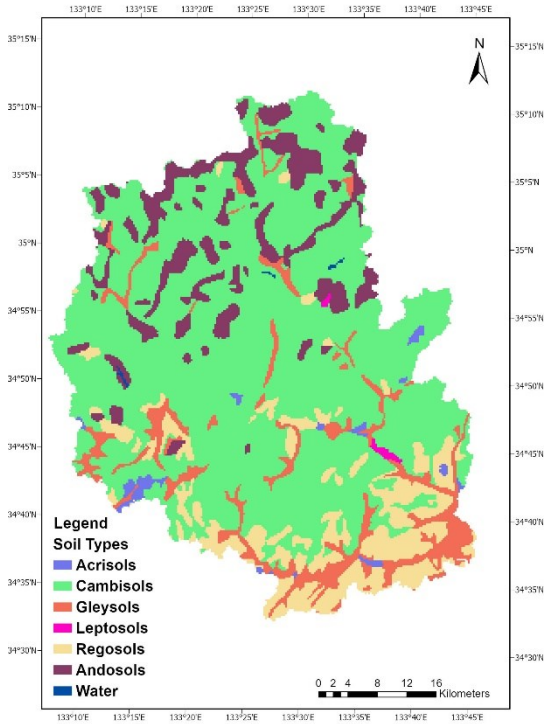

Figure 5 Soil types of Takahashi catchment

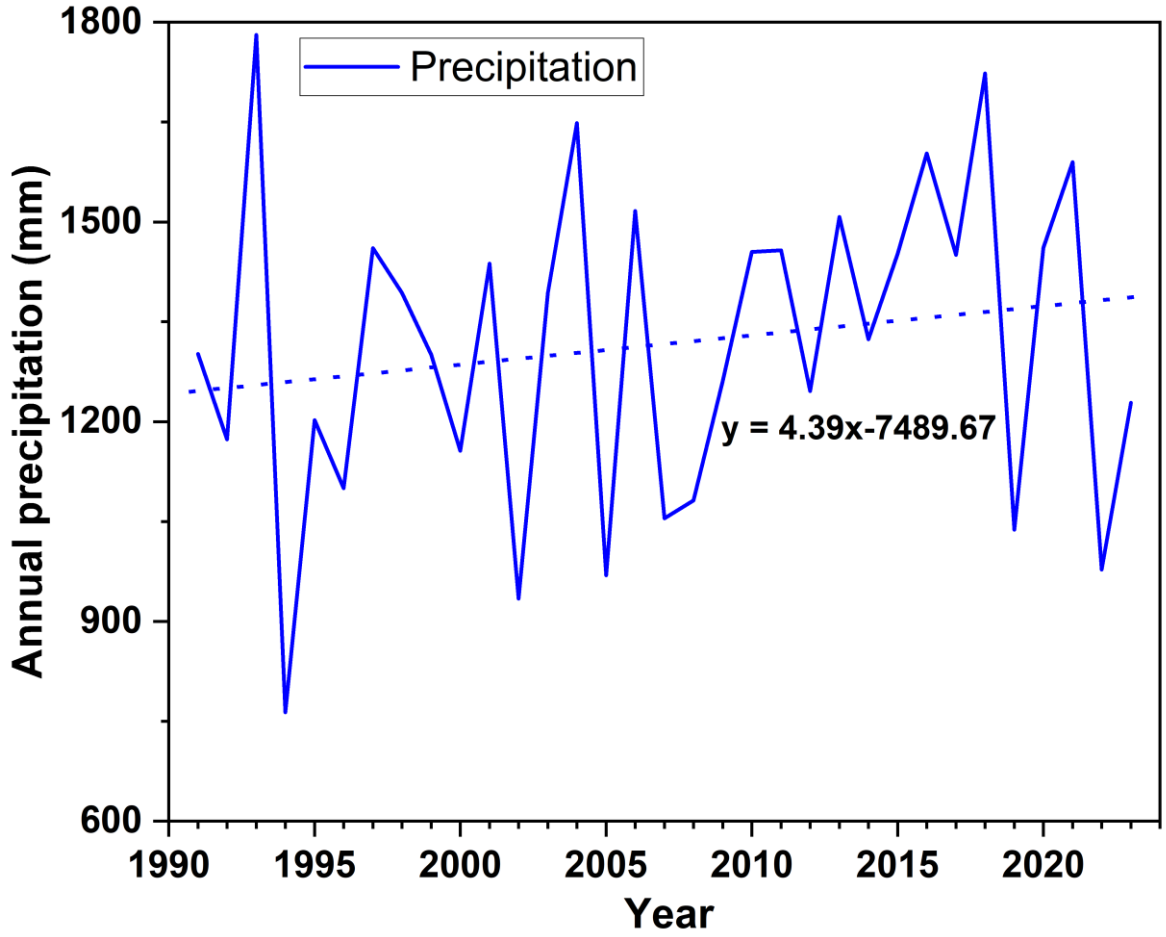

Figure 6 Average annual precipitation across Takahashi catchment

The Takahashi catchment's geological setting is 58.3% igneous rock, 36.5% sedimentary rock, and 5.2% metamorphic rock. Based on the Ministry of Land, Infrastructure, Transport and Tourism (MLIT) classification, the Takahashi catchment's geology has 13 subcategories, with granite and rhyolite composing 44% of the catchment area (Figure 7). The studied catchment has limestone areas, mainly in parts of the Takahashi and Nariwa tributaries.

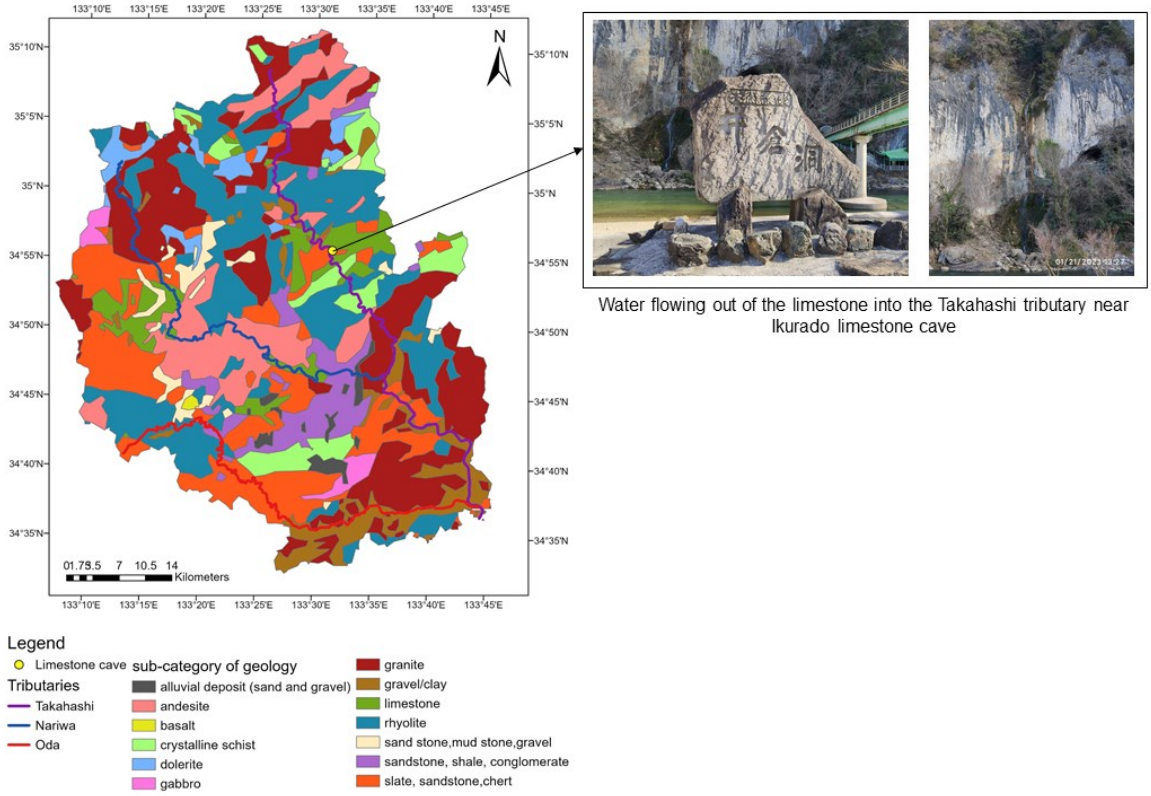

Figure 7 Outcrop geology of Takahashi catchment

The studied catchment experienced a devastating flood disaster in 2018 due to the significant amount of cumulative precipitation over 48 hours rather than the rainfall intensity per hour (Nishimura et al., 2020). Shakti et al. (2020) proved that the Rainfall–Runoff–Inundation (RRI) model is suitable for evaluating the flood inundation analysis of flood-prone river basins, including the Oda tributary of the Takahashi River system. Meanwhile, Nihei et al. (2019) compared the flooding situation of the Oda River in Okayama Prefecture in 2018 and the Kinugawa River in the Ibaraki Prefecture in 2015. Although the Kinugawa River's inundation area was four times that of the Oda River, the inundation volume was similar because the inundation depth of the Oda River was 5.38 m, which was greater than that of the Kinugawa River at 3.01 m. Along with heavy

rainfall and flooding, major rivers in the Okayama Prefecture experienced high sediment yield (Nishimura et al., 2020).

The Takahashi catchment's geographical setting, with its climatic and vulnerable conditions, provides an ideal condition for studying sediment dynamics in steep slope catchments and the impacts of extreme weather events on flood-related disasters. Finer temporal resolutions are favourable for modelling high-flow events, however, data scarcity, especially for sediment, limits high-temporal modelling research (Jeong et al., 2011; Tan et al., 2020). Therefore, the availability of hourly observed data for the Takahashi catchment offers optimal conditions for studying high-flow events in sediment transport.

2.2 Soil and water assessment tool

SWAT is a semi-distributed, continuous time-scale model developed by the United States Department of Agriculture (USDA) Agricultural Research Service. The model is used to assess the impacts of land management practices on hydrological components and water quality and has been successfully applied to small and continental scales. It is widely used in large, complex watersheds for simulating long-term impacts therein (Arnold et al., 2012). SWAT requires topography, soil property, land use, and meteorological data, such as precipitation, maximum and minimum air temperature, relative humidity, wind speed, and solar radiation, as input data for the simulation of hydrological components at different time steps. SWAT detaches catchments into subbasins. Subbasins are then dissociated into hydrological response units (HRUs). An HRU is a unit formed by homogeneous land use, soil, and topography (Neitsch et al., 2011).

SWAT divides the hydrological cycle into a land phase and a routing phase. The land phase computes the hydrological balance and sediment yields on a daily scale. The land phase of the hydrologic cycle of the SWAT model is based on the water balance equation described in Eq (1):

$$SW_t = SW_0 + \sum_{i=1}^{t}(R_{day} - Q_{surf} - E_a - w_{seep} - Q_{gw}) \quad (1)$$

where SW_t is the final soil water content ($\mathrm{mmH_2O}$), SW_0 is the initial soil water content ($\mathrm{mm\,H_2O}$), t stands for time (days), R_{day} is the amount of precipitation on day i ($\mathrm{mmH_2O}$), Q_{surf} is the amount of surface runoff on day i ($\mathrm{mmH_2O}$), w_{seep} is the amount of percolation and bypass flow exiting the soil profile bottom on day i ($\mathrm{mmH_2O}$), and Q_{gw} is the amount of return flow on day i ($\mathrm{mmH_2O}$).

SWAT provides two options for simulating the infiltration and surface runoff: the SCS Curve Number method and the Green and Ampt Mein Larson method. SCS Curve Number is an empirical model used for the daily time step, while Green and Ampt Mein Larson is a physically-based model used for the sub-daily time step. SWAT can perform hydrologic routing with two main methods: variable storage routing and Muskingum routing methods. Variable storage routing considers the outflow volume assigned as the total inflow volume and storage volume. The Muskingum routing method calculates the storage volume as the combination of the wedge and prism storage in the channel, which is a suitable routing method for high-flow flood events. In SWAT, the upland soil erosion is calculated by the empirically developed MUSLE equation on a daily scale, whereas the splash erosion model considering the soil detachment by rain drop's kinetic energy is used to simulate a sub-daily scale erosion. Detailed sub-daily sediment simulation algorithms are provided in Jeong et al. (2011).

2.3 Assessment of model performances

The coefficient of determination (R^2) and Nash–Sutcliffe efficiency (NSE) are widely used statistical indexes for assessing the accuracy of model simulations (Aloui et al., 2023; Bressiani et al., 2015; Gassman et al., 2007; Gassman et al., 2014; Tan et al., 2019; Tan et al., 2020; Tuppad et al., 2011; Verma et al., 2022). R^2 shows the degree of linearity between observed and simulated data and ranges from 0 to 1. If its value is closer to 1, the simulated data have a good agreement with the observed data. Meanwhile, NSE is a normalized statistic that assesses the relative amount of residual variance in comparison with the measured data variance. NSE can take measurement uncertainty into account and is good for use with continuous long-term simulations and can be used to assess how well a model simulates trends for the output response of concern. Furthermore, percent bias (PBIAS) is used to determine the average model simulation bias. Positive PBIAS values indicate underestimation, whereas negative values indicate overestimation. PBIAS is recommended for use with other statistical indicators to determine a model's performance (Moriasi et al., 2015). The equations for R^2, NSE, and PBIAS are expressed in Eqs (3)–(5), respectively:

$$R^2 = \frac{[\sum_{i=1}^{n}(O_i-\bar{O})(P_i-\bar{P})]^2}{\sum_{i=1}^{n}(O_i-\bar{O})^2 \sum_{i=1}^{n}(P_i-\bar{P})^2} \quad (3)$$

$$NSE = 1 - \frac{\sum_{i=1}^{n}(O_i-P_i)^2}{\sum_{i=1}^{n}(O_i-\bar{O})^2} \quad (4)$$

$$PBIAS = 100 \times \frac{\sum_{i=1}^{n} O_i-P_i}{\sum_{i=1}^{n} O_i} \quad (5)$$

where O_i represents the observed data, P_i represents the simulated data, $\bar{O}$ is the mean of the observed data, and $\bar{P}$ is the mean of the simulated data. The model performance evaluation criteria reported in Moriasi et al., (2015) are tabulated in Table 2.

Table 2 Model performance evaluation criteria stated in Moriasi et al. (2015)

Statistical indices	Output	Very Good	Good	Satisfactory	Not Satisfactory
R^2	streamflow	$R^2 > 0.85$	$0.75 < R^2 \leq 0.85$	$0.6 < R^2 \leq 0.75$	$R^2 \leq 0.6$
	sediment	$R^2 > 0.8$	$0.65 < R^2 \leq 0.8$	$0.4 < R^2 \leq 0.65$	$R^2 \leq 0.4$
NSE	streamflow	NSE > 0.8	0.7 < NSE ≤ 0.8	0.5 < NSE ≤ 0.7	NSE ≤ 0.5
	sediment	NSE > 0.8	0.7 < NSE ≤ 0.8	0.45 < NSE ≤ 0.7	NSE ≤ 0.45
PBIAS	streamflow	PBIAS < ±5	±5 < PBIAS ≤ ± 10	±10 < PBIAS ≤ ± 15	PBIAS ≥ ± 15
	sediment	PBIAS < ±10	±10 < PBIAS ≤ ± 15	±15 < PBIAS ≤ ± 20	PBIAS ≥ ± 20

Note: These criteria are set for streamflow at daily, monthly, and annual scales and the sediment at a monthly scale.

2.4 References

Aloui, S., Mazzoni, A., Elomri, A., Aouissi, J., Boufekane, A., & Zghibi, A. (2023). A review of Soil and Water Assessment Tool (SWAT) studies of Mediterranean catchments: Applications, feasibility, and future directions. Journal of Environmental Management (Vol. 326). Academic Press. https://doi.org/https://doi.org/10.1016/j.jenvman.2022.116799

Arnold, J. G., Moriasi, D. N., Gassman, P. W., Abbaspour, K. C., White, M. J., Srinivasan, R., Santhi, C., Harmel, R. D., Van Griensven, A., Liew, M. W. Van, Kannan, N., Jha, M. K., Harmel, D., Member, A., Liew, M. W. Van, & Arnold, J.-F. G. (2012). SWAT: model use, calibration, and validation. Transactions of the ASABE, 55(4), 1491–1508. http://swatmodel.tamu.edu

Bressiani, D. de A., Gassman, P. W., Fernandes, J. G., Garbossa, L. H. P., Srinivasan, R., Bonumá, N. B., & Mendiondo, E. M. (2015). A review of soil and water assessment tool (SWAT) applications in Brazil: Challenges and prospects. International Journal of Agricultural and Biological Engineering, 8(3), 1–27. https://doi.org/10.3965/j.ijabe.20150803.1765

Gassman, P. W., Reyes, M. R., Green, C. H., Arnold, J. G., & Gassman, P. W. (2007). The Soil and Water Assessment Tool: Historical Development, Applications, and Future Research Directions. Transactions of the ASABE, 50(4), 1211–1250.

Gassman, P. W., Sadeghi, A. M., & Srinivasan, R. (2014). Applications of the SWAT Model Special Section: Overview and Insights. Journal of Environmental Quality, 43(1), 1–8. https://doi.org/10.2134/jeq2013.11.0466

Jeong, J., Kannan, N., Arnold, J. G., Glick, R., Gosselink, L., Srinivasan, R., & Harmel, R. D. (2011). Development of sub-daily erosion and sediment transport algorithms for SWAT. Transactions of the ASABE, 54(5), 1685–1691. https://doi.org/10.13031/2013.39841

Moriasi, D. N., Gitau, M. W., Pai, N., & Daggupati, P. (2015). Hydrologic and water quality models: Performance measures and evaluation criteria. Transactions of the ASABE, 58(6), 1763–1785. https://doi.org/10.13031/trans.58.10715

Neitsch, S. L., Arnold, J. G., Kiniry, J. R., & Williams, J. R. (2011). Soil and Water Assessment Tool Theoretical Documentation Version 2009.

Nihei, Y., Shinohara, A., Ohta, K., Maeno, S., Akoh, R., Akamatsu, Y., Komuro, T., Kataoka, T., Onomura, S., & Kaneko, R. (2019). Flooding along Oda river due to the western Japan heavy rain in 2018. Journal of Disaster Research, 14(6), 874–885. https://doi.org/10.20965/jdr.2019.p0874

Nishimura, S., Takeshita, Y., Nishiyama, S., Suzuki, S., Shibata, T., Shuku, T., Komatsu, M., & Kim, B. (2020). Disaster report of 2018 July heavy rain for geo-structures and slopes in Okayama. Soils and Foundations, 60(1), 300–314. https://doi.org/10.1016/j.sandf.2020.01.009

Shakti, P. C., Kamimera, H., & Misumi, R. (2020). Inundation analysis of the Oda River Basin in Japan during the flood event of 6-7 July 2018 utilizing local and global hydrographic data. Water, 12(4). https://doi.org/10.3390/W12041005

Tan, M. L., Gassman, P. W., Srinivasan, R., Arnold, J. G., & Yang, X. (2019). A Review of SWAT Studies in Southeast Asia: Applications, Challenges and Future Directions. Water, 11(5), 914. https://doi.org/10.3390/w11050914

Tan, M. L., Gassman, P. W., Yang, X., & Haywood, J. (2020). A review of SWAT applications, performance and future needs for simulation of hydro-climatic extremes. Advances in Water Resources (Vol. 143). https://doi.org/10.1016/j.advwatres.2020.103662

Tuppad, P., Douglas-Mankin, K. R., Lee, T., Srinivasan, R., Arnold, J. G., Srinivasan, R., & Member, A. (2011). Soil and Water Assessment Tool (SWAT) Hydrologic/Water Quality Model: Extended Capability and Wider Adoption. Transactions of the ASABE, 54(5), 1677–1684.

Verma, S. K., Prasad, A. D., & Verma, M. K. (2022). An Assessment of Ongoing Developments in Water Resources Management Incorporating SWAT Model: Overview and Perspectives. Nature Environment and Pollution Technology, 21(4), 1963–1970. https://doi.org/10.46488/NEPT.2022.v21i04.051

Wang, K., Onodera, S., Saito, M., Shimizu, Y., & Iwata, T. (2022). Effects of forest growth in different vegetation communities on forest catchment water balance. Science of the Total Environment, 809. https://doi.org/10.1016/j.scitotenv.2021.151159

Chapter 3 Annual and spatial variations of sediment yield

3.1 Background and objectives

The inner region of Southwest Japan is often damaged by slope failures and debris flow disasters, whereas the outer region of Southwest Japan is common to typhoon-induced deep-seated landslides owing to the difference in geology (Hayashi et al., 2022). Several studies reported that the torrential rainfall occurred in western Japan in 2018 July, created severe flooding and sediment disasters, particularly in many river basins of Hiroshima and Okayama prefectures (Yoshida, 2018; Amano et al., 2021; Nihei et al., 2019; Shakti & Kamimera, 2019; Nishimura et al., 2020; Nohara et al., 2020; Shakti et al., 2020). Ministry of Land, Infrastructure, Transport, and Tourism (MLIT) reported 2581 occurrences of sediment disasters in the heavy rainfall of July 2018, nearly 2.5 times the annual average and primarily in western Japan (Hayashi et al., 2022).

According to a survey report from the Japanese government cabinet office (2020), the most serious water-related problem due to climate change is frequent floods and landslides. Consequently, the respondents wish for the government to focus on developing flood and sediment disaster prevention facilities. MLIT gives precise forecasts for a few hours ahead of flooding based on the upstream water level. Although forecasts have improved, it is not always possible to predict the exact timing of the rain that triggers these climate-related disasters (Disaster Management Bureau, 2018). When residents go to evacuate, there are often few hours between the forecast and the evacuation, or the evacuation has already become challenging owing to severe rain. The immediate evacuation action becomes more difficult especially if it happens to be at late night (Ma

et al., 2021; Nohara et al., 2020). This highlighted the importance of early alarm systems for flood and flood-related disasters like sediment disasters.

Policymakers require information on the extent and place of disasters when setting sediment disaster countermeasures (de Vente et al., 2006). Because sediment budgets are site-specific, both spatial and temporal variations of sediment transport are important for understanding the sediment transport mechanisms from headwaters to river channels (Wang J. et al., 2022). Subsequently, identifying sediment hotspot areas is crucial for the prevention of and planning and preparedness for flood and sediment disasters. Further, understanding the location and scope of erosions is essential to achieving the UN SDGs and the UN strategies for soil conservation (Borrelli et al., 2020).

In this study, we aim to evaluate the SWAT model's applicability to simulate streamflow and suspended sediment yield in a steep, geologically complex forested catchment, identify high-sediment-contribution areas in the catchment susceptible to sediment disasters, and assess the sediment yield variations between dry and wet years.

3.2 Materials and method

3.2.1 Data collection and model implementation

SWAT 2012 (Rev. 685) along with a QGIS interface simulated the daily streamflow and sediment load from 2002 to 2007 in this study. The basic data input for topography was derived from the National Aeronautics and Space Administration’s 30-m Shutter Radar Topography Mission Digital Elevation Model (DEM). DEM was used to delineate the stream network and the catchment, and derive the slope of the terrain. High-resolution with 10-m land use data for 2006 from the Japan Aerospace Exploration

Agency was used for land use input. Soil data were obtained from MLIT. The daily meteorological data from 11 weather stations, as shown in Figure 2, (11 stations for precipitation, 6 stations for temperature, relative humidity, solar radiation, and wind speed) surrounding the catchment obtained from the Japan Meteorological Agency and the National Agriculture and Food Research Organization were input into the model. Moreover, water management policies in watersheds, including reservoirs, are important for model accuracy (K. Wang et al., 2021). Although several reservoirs stand on the branches of the Takahashi and Nariwa tributaries, the Chiya and Koumoto reservoirs on the upstream of the Takahashi tributary and the Shin-nariwa reservoir on the Nariwa tributary were considered because of their locations, water storage capacity, and data availability (Figure 2).

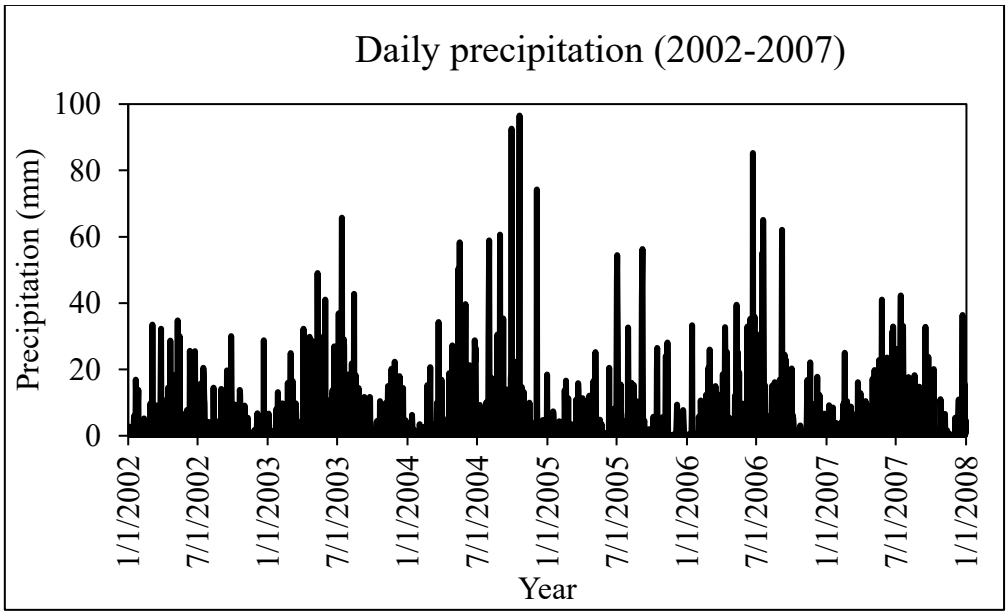

Figure 8 Daily precipitation during the calibration and validation years

The study area was divided into 27 subbasins and 2689 HRUs. In creating HRUs, four slope bands were set (<15%, 15%–30%, 30%–45%, and >45%). The model had a three-year warm-up period, and the simulated model was calibrated from 2002 to 2004

and validated from 2005 to 2007. The daily precipitation during the calibration and validation years are as shown in Figure 8. Based on the long-term mean precipitation data, the model simulation years could be categorized into dry years (2002, 2005, and 2007) and wet years (2003, 2004, and 2006). Leta et al. (2017) suggested that simultaneous multisite calibration is preferable in catchments with large spatial variations of soils, land uses, and geology, which consequently have spatial differences in streamflow-generating processes. Because Takahashi is a catchment with high spatial heterogeneities, the daily observed streamflow data from three hydrological stations (Sakazu, Yagata, and Hiwa) and daily observed sediment data from the Sakazu station were used for calibration and validation. The streamflow observed data were acquired from MLIT, and the sediment data were obtained from the Okayama River Management Office. The potential evapotranspiration was applied using the Penman–Monteith method, and the stream channel sediment routing was performed using the simplified Bagnold equation in this study. The model was calibrated and validated using the auto calibration SWAT-CUP SPE program considering the sensible water balance components of the catchment and the observed data.

3.3 Results and discussions

3.3.1 Parameterization and model performance assessment

According to the literature and calibration manual, eleven parameters for streamflow and seven parameters for sediment were selected for calibration (Abbaspour et al., 2015; Arnold et al., 2012; Ashine & Tadesse Bedane, 2022). The calibrated parameters and the best-fit values are tabulated in Table 3.

Table 3 Calibrated parameters for daily streamflow and sediment

	Modification type	Parameter Name	Description	Minimum	Maximum	Fitted	Remark
Flow	r	CN2	SCS runoff curve number	-0.2	0.1	-0.018	FRSD
						0.04	FRSE
						-0.05	GRAS, RICE
						-0.1	AGRL
						-0.159	BARR
						-0.2	URBN
	v	RCHRG_DP	Deep aquifer percolation fraction	0.25	0.35	0.31	
	v	ESCO	Soil evaporation compensation factor	0.15	0.8	0.181	FRSD, FRSE
						0.675	AGRL, RICE
						0.66	GRAS
						0.8	BARR, URBN
	r	SOL_K	Saturated hydraulic conductivity	-0.2	0.2	-0.098	
	r	SOL_AWC	Available water capacity of the soil layer	-0.2	0.2	0.011	
	r	SOL_BD	Moist bulk density	-0.2	0.2	0.018	
	v	GWQMN	Threshold depth of water in the shallow aquifer required for the return flow to occur (mm)	150	3000	200*	1-5,10-21,24-27
						2000	6-9
						3000	22,23
	v	CH_N2	Manning's "n" value for the main channel	0.02	0.1	0.069	1-5,10-21,24-27
						0.055	6-9
						0.068	22,23
	v	ALPHA_BF	Baseflow alpha factor (days)	0.2	0.7	0.375	
	r	HRU_SLP	Average slope steepness	-0.35	-0.1	-0.28	

	Modification type	Parameter Name	Description	Minimum	Maximum	Fitted	Remark
	v	CANMAX	Maximum canopy storage	5	25	11.2	
Sediment	v	CH_COV1	Channel erodibility factor	0.01	0.06	0.037	
	v	CH_COV2	Channel cover factor	0.01	0.1	0.057	
	v	USLE_P	Support practice factor	0	0.5	0.005	
	r	USLE_C	Minimum USLE cover factor	-0.25	0.25	0.018	RICE
						0.01	FRSD, FRSE, GRAS
	r	PRF_BSN	Peak rate adjustment factor for sediment routing in the main channel	0	1	0.85	
	v	SPCON	Linear parameter for calculating the maximum amount of sediment that can be reentrained during channel sediment routing	0.001	0.01	0.009	
	v	SPEXP	Exponent parameter for calculating sediment reentrained during channel sediment routing	1	1.5	1.39	

Note: r indicates that the parameter value is changed relatively, and v indicates that the default parameter is replaced, * represents the value for limestone-influenced subbasins.

During the calibration stage, Manning's “n” roughness of the main channel (CH_N2) and threshold depth of water in the shallow aquifer required for the return flow

to occur (GWQMN) variably depending on the tributary, and the SCS runoff curve number (CN2) and soil evaporation compensation factor (ESCO) showed variations between different land use types. Groundwater flow from the shallow aquifer to the river occurred when the GWQMN values were lower than or equal to the water depth in the shallow aquifer. The Takahashi and Nariwa tributaries were limestone-influenced areas. According to the observed data from Hiwa station, the model was calibrated to have an increased shallow aquifer flowing into the Takahashi and Nariwa tributaries by setting a low GWQMN value of 200. The Oda tributary and subbasins 22 and 23, which are close to the outlet of the Takahashi River into the Seto inland sea, showed the highest GWQMN values (2,000 and 3,000, respectively). Wang et al. (2019) stated that the karst structures in limestone areas have great permeability and make underground runoff more prevalent than surface runoff. Consequently, the water cycle in limestone environments differs from that in non-limestone areas.

Table 4 Statistical performance of the SWAT model for calibration (2002 - 2004) and validation (2005 - 2007)

Stations	Hiwa		Yagata		Sakazu (streamflow)		Sakazu (Sediment)	
Index	calibration	validation	calibration	validation	calibration	validation	calibration	validation
NSE	0.68	0.69	0.62	0.57	0.7	0.64	0.46	0.47
R^2	0.74	0.73	0.68	0.68	0.73	0.68	0.55	0.48
PBIAS	14.7	9.2	14.7	8.9	-8	-14.8	14.3	-19.7

The statistical indexes for the model calibration and validation years, as shown in Table 4, were satisfactory, according to Moriasi et al. (2015). The calibration year for

streamflow resulted in NS values of 0.61, 0.68, and 0.7 and validation values of 0.56, 0.7, and 0.65 for the Yagata, Hiwa, and Sakazu stations, respectively. Sediment calibration and validation NS values at Sakazu station were 0.49 and 0.46, respectively. According to the PBIAS values, the model underestimated the streamflow of Yagata and Hiwa and overestimated that for Sakazu. The sediment PBIAS showed that the model underestimated the sediment for the calibration years and overestimated that for the validation years.

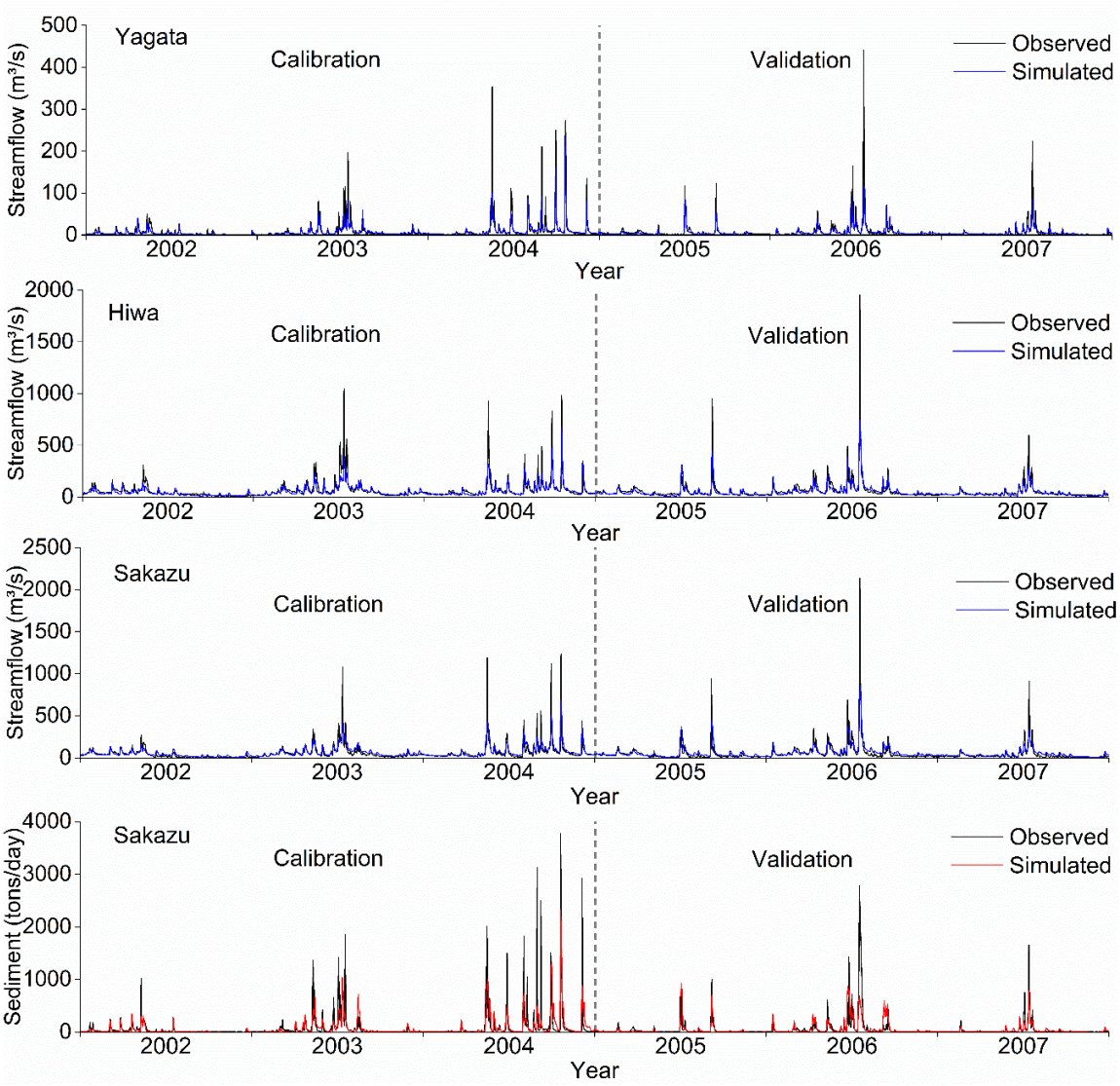

Figure 9 Calibrated and simulated daily streamflow and sediment

Figure 9 shows the goodness of fit between the observed and simulated streamflow and sediment yield. The year 2004 had a unique precipitation period among all the simulated years. Generally, the studied area receives heavy rain in summer when typhoons occur. However, 2004 had a prolonged rainy period, which started from the end of spring to early autumn. The model underestimated the sediment in calibration years, which could be due to the prolonged rainy period. Some of the peaks in the figure did not completely match. This part of the flow can be considered as the water discharged into the river through the drainage system during the period. As the drainage system usually responds very quickly, this leads to a higher peak value (Wang K. et al., 2021). Overall, the results of the model are credible.

3.3.2 Water balance components

The SWAT model can estimate the water balance components of the catchment. The overall water balance components of the Takahashi catchment in relation to precipitation were found to be evapotranspiration (42%), return flow (18%), lateral flow (17%), surface runoff (15%), and deep aquifer recharge (8%). The annual water balance components showed that the high precipitation years 2004 and 2006 had a higher contribution of surface runoff to streamflow than the remaining years (Figure 10b). Seasonally, summer received the highest precipitation mainly due to the occurrence of typhoons and showed relatively higher evapotranspiration and surface runoff. The lowest evapotranspiration and surface runoff occurred in winter, owing to the season's low precipitation and average temperature (Figure 10a).

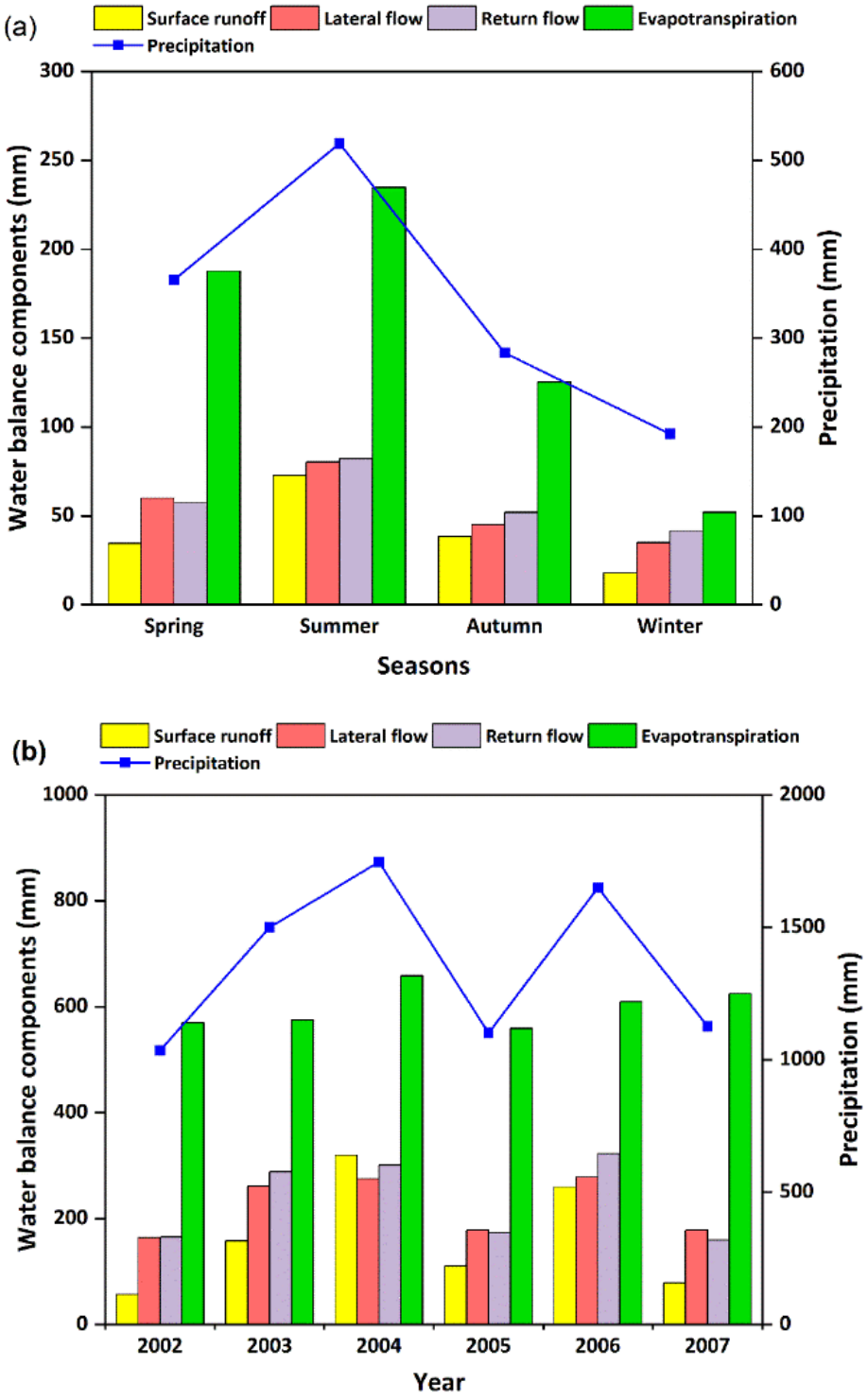

Figure 10 Water balance components (a) seasonal, (b) annual

3.3.3 Annual and seasonal variations of sediment load

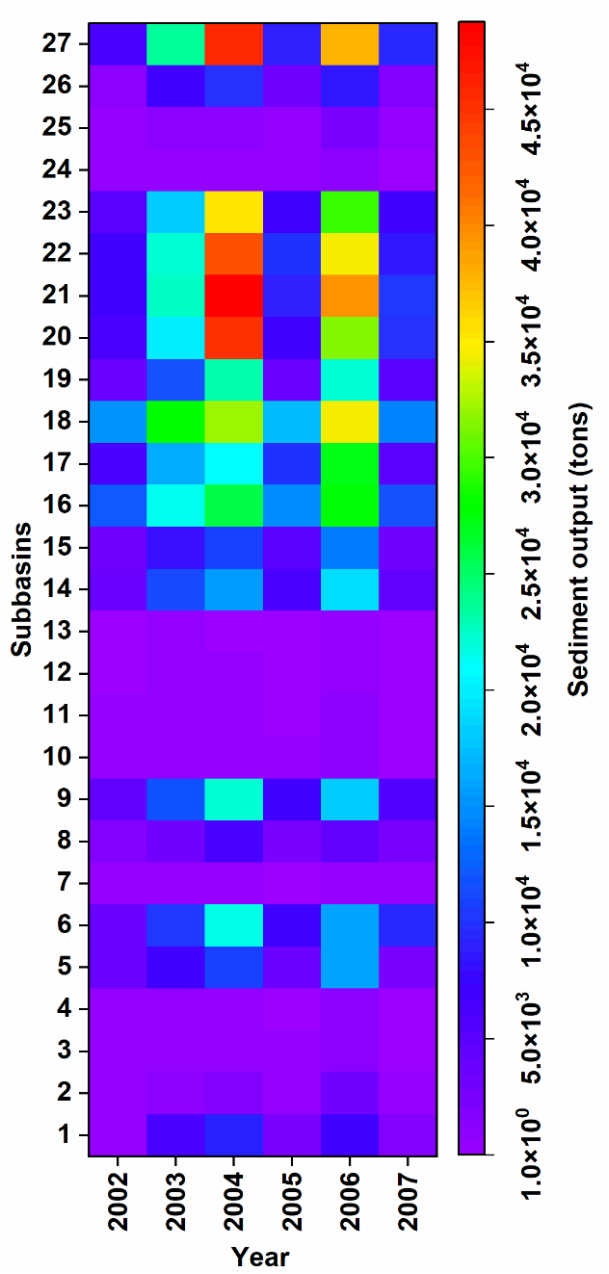

Figure 11 Annual sediment output variations by subbasins

Figure 11 shows the sediment output variations by subbasins. Among the 27 subbasins, 10 exhibited slight changes in sediment output over the years, and 17 (particularly subbasins 20, 21, 22, and 27) showed pronounced fluctuations. Although subbasins 16 and 18 showed a high sediment output throughout the years, subbasins 20,

21, 22, and 27 showed the highest sediment output in wet years. The subbasins with consistently low sediment output are located in the Takahashi tributary headwater regions, whereas those with the highest fluctuations are located in the Nariwa tributary.

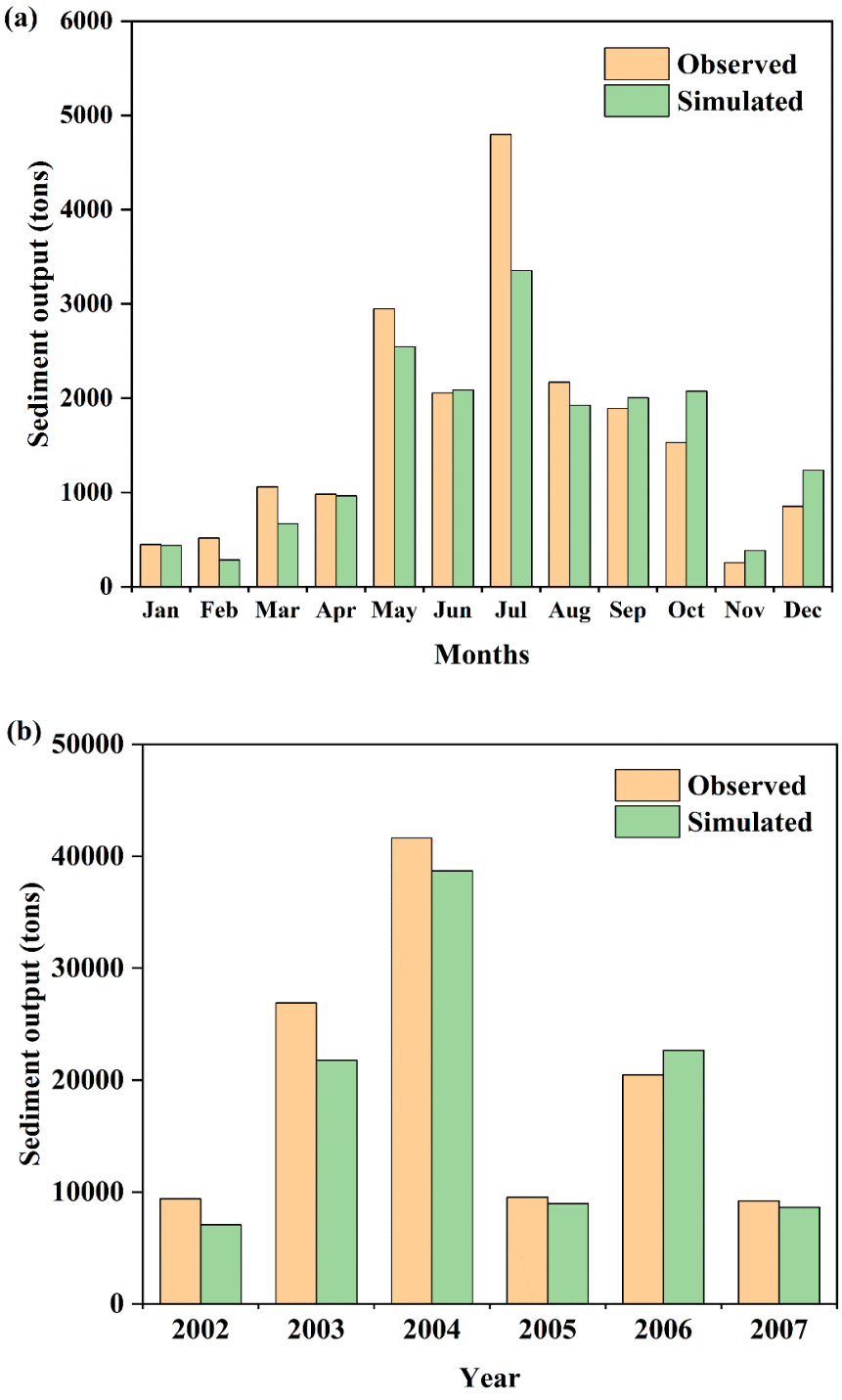

Figure 12 Sediment output variations (a) monthly, (b) annually

The annual average observed sediment output was 19,518.6 tons yr^{-1}, while the simulated value was 17,974.5 tons yr^{-1}, reflecting an 8% underestimation by the model. However, the observed and modeled sediment outputs were comparable regardless of this difference. The sediment load showed a high correlation with the total precipitation and the precipitation pattern and intensity. Sediment transport peaked from late spring to mid-autumn (May–September) (Figure 12a). Among the wet years, 2004 is unique with a prolonged rainy period, having the highest sediment output (38,705.5 tons) and precipitation (1,755 mm) (Figure 12b). High precipitation was also recorded in 2006 (1,652 mm) and 2003 (1,503 mm), and the simulated sediment output was 22,665.7 and 21,781.5 tons, respectively, which are considerably lower than that recorded in 2004 and implies that sediment production is influenced by precipitation patterns and intensities, leading to variations even in years with comparable total precipitation.

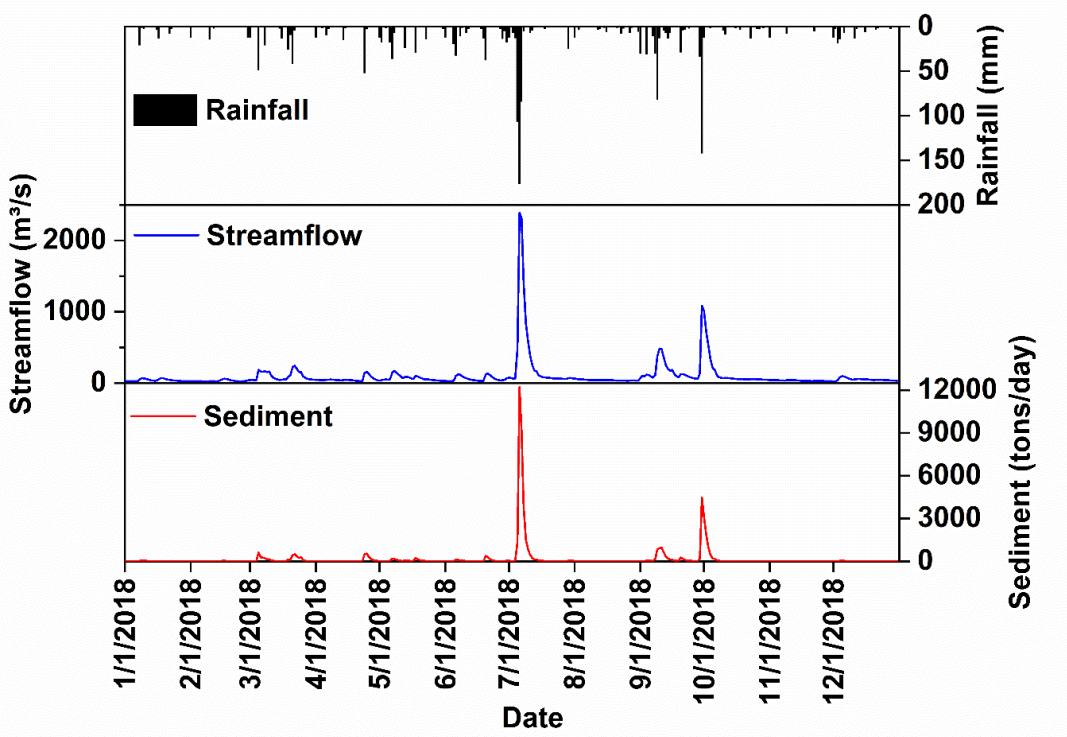

Figure 13 Simulated daily sediment load of 2018

The calibrated model was used to simulate the year 2018, which experienced a devastating flooding disaster (Figure 13). During this catastrophic event, the daily precipitation reached 177 mm. The model successfully captured the extreme precipitation event, simulating a peak sediment output of 12,220 tons on July 6. This peak sediment output was higher than the annual sediment load during dry years, which is typically less than 10,000 tons.

3.3.4 Spatial variation of sediment yield

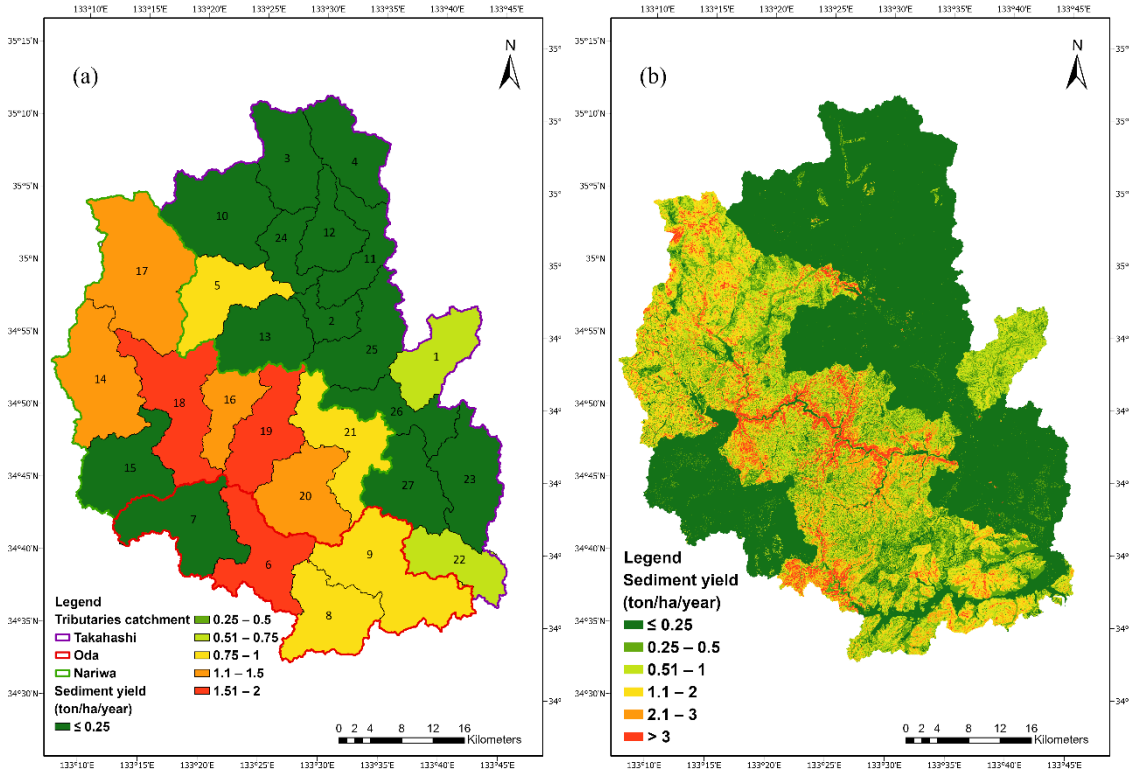

Figure 14 Sediment yield spatial variations by (a) subbasins, (b) HRUs

The simulated average annual sediment yield of the catchment was 0.55 tons ha^{-1} yr^{-1}. The average annual spatial variation of the sediment yield per subbasin is shown in Figure 14(a). The Takahashi tributary subbasins showed the most negligible sediment

yield among the three main tributaries. Except for the subbasins 1 and 5, Takahashi tributary subbasins have sediment yields <0.25 tons ha^{-1} yr^{-1}. Meanwhile, the Nariwa and Oda tributary subbasins have moderate to the highest sediment yield, ranging 0.75–2 tons ha^{-1} yr^{-1}, except for the subbasin 7 and 15 with sediment yield values of <0.25 tons ha^{-1} yr^{-1}. In subbasins with high sediment yield, the hotspot areas mainly include HRUs located along the river channel (Figure 14b). It turned out that the steep slopes (>60%) along the river channel, particularly in the Nariwa tributary, were these high sediment yield areas.

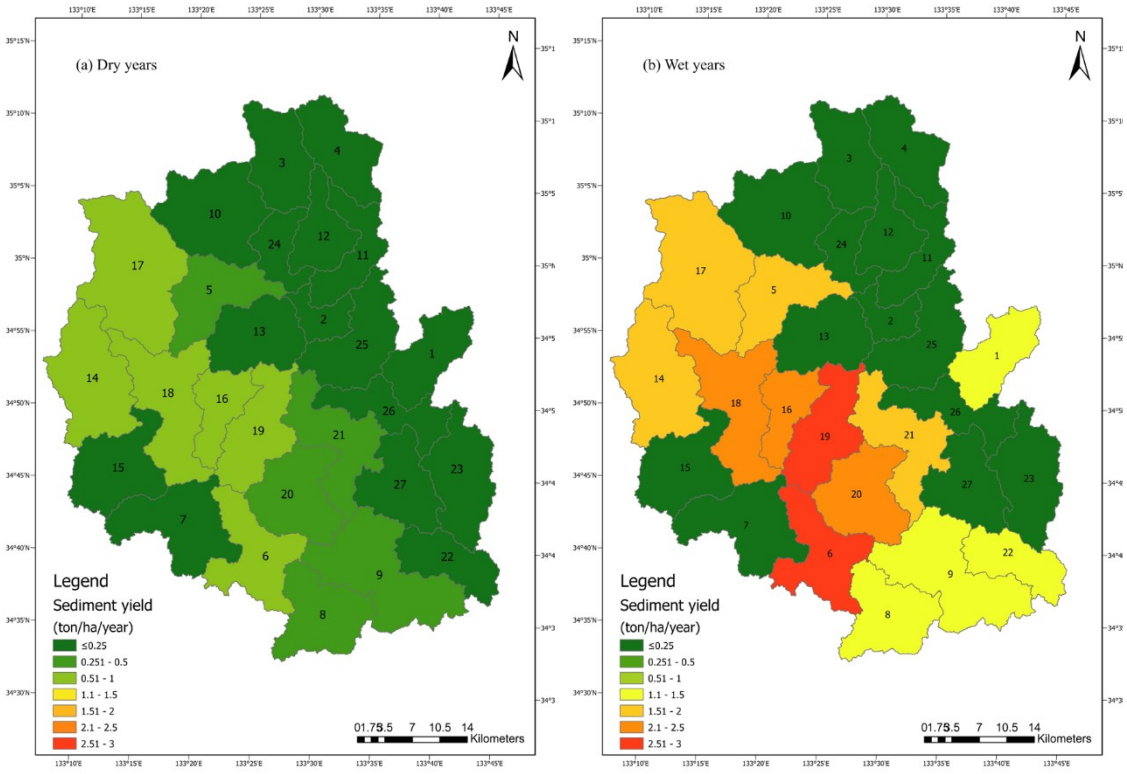

Figure 15 Spatial variations of sediment yield in (a) dry years, (b) wet years

The average annual sediment yield variation between dry and wet years was significant with 0.24 ton ha^{-1} yr^{-1} in dry years and 0.9 ton ha^{-1} yr^{-1} in wet years. In dry years, the studied catchment's sediment yield was <1 ton ha^{-1} yr^{-1} (Figure 15a), while it

increased substantially in wet years, reaching up to 3 ton ha^{-1} yr^{-1} in subbasins 6 and 19 (Figure 15b). The Takahashi tributary exhibited less variation compared to the Oda and Nariwa tributaries. The sediment yield in the Nariwa and Oda tributary subbasins, increased drastically to 1.1–3 ton ha^{-1} yr^{-1} in wet years, from 0.25 and 1 ton ha^{-1} yr^{-1} in dry years. Subbasins 6 and 19 are the most critical subbasins under high precipitation as their sediment yield in wet years is nearly threefold of that in the dry years.

3.4 Conclusions

The study examined the detailed annual and spatial variations of sediment yield in the steep, geologically complex, forested Takahashi River catchment. The SWAT model is found to be a reliable tool for simulating streamflow and sediment yield, with satisfactory calibration and validation results at multiple hydrological stations. The distinct geological and topographical features of the Takahashi catchment significantly influenced the catchment's hydrology and sediment yield variations.

The results showed that sediment yield is highly sensitive to annual precipitation patterns and intensity, with wet years producing significantly higher sediment loads compared to dry years. The steep slope along the river channels, particularly in the Nariwa tributary, were identified as sediment hotspots. These areas exhibited pronounced fluctuations in sediment output, highlighting the need for targeted sediment disaster prevention measures.

This study contributes valuable insights into sediment transport mechanisms, which are crucial for developing comprehensive flood and high-sediment-yield prevention plans. By understanding sediment dynamics and spatial variations, we can

better prepare for and mitigate the impacts of extreme weather events, contributing to the sustainability and resilience of vulnerable regions.

3.5 References

Abbaspour, K. C., Rouholahnejad, E., Vaghefi, S., Srinivasan, R., Yang, H., & Kløve, B. (2015). A continental-scale hydrology and water quality model for Europe: Calibration and uncertainty of a high-resolution large-scale SWAT model. Journal of Hydrology, 524, 733–752. https://doi.org/10.1016/j.jhydrol.2015.03.027

Amano, T., Asai, K., Shirozu, H., Takabu, A., & Yamamoto, T. (2021). Influence of sediment discharge and driftwoods on Noro-gawa dam and river flooding during heavy rain in July 2018.

Arnold, J. G., Kiniry, J. R., Srinivasan, R., Williams, J. R., Haney, E. B., & Neitsch, S. L. (2012). Input/Output Documentation Soil & Water Assessment Tool.

Ashine, E. T., & Tadesse Bedane, M. (2022). Most Sensitive Parameters of Soil and Water Assessment Tool (SWAT) Hydrological Model: A Review. Advances in Oceanography & Marine Biology, 3(2). https://doi.org/10.33552/AOMB.2022.03.000558

Borrelli, P., Robinson, D. A., Panagos, P., Lugato, E., Yang, J. E., Alewell, C., Wuepper, D., Montanarella, L., & Ballabio, C. (2020). Land use and climate change impacts on global soil erosion by water (2015-2070). Proceedings of the National Academy of Sciences, 117(36), 21994–22001. https://doi.org/10.1073/pnas.2001403117

de Vente, J., Poesen, J., Bazzoffi, P., Rompaey, A. Van, & Verstraeten, G. (2006). Predicting catchment sediment yield in Mediterranean environments: the importance of sediment sources and connectivity in Italian drainage basins. Earth Surface Processes and Landforms, 31(8), 1017–1034. https://doi.org/10.1002/esp.1305

Hayashi, S. I., Kunitomo, M., Mikami, K., & Suzuki, K. (2022). Recent and Historical Background and Current Challenges for Sediment Disaster Measures against Climate Change in Japan. Water (Vol. 14, Issue 15). https://doi.org/10.3390/w14152285

Leta, O. T., van Griensven, A., & Bauwens, W. (2017). Effect of Single and Multisite Calibration Techniques on the Parameter Estimation, Performance, and Output of a SWAT Model of a Spatially Heterogeneous Catchment. Journal of Hydrologic Engineering, 22(3). https://doi.org/10.1061/(ASCE)HE.1943-5584.0001471

Ma, W., Ishitsuka, Y., Takeshima, A., Hibino, K., Yamazaki, D., Yamamoto, K., Kachi, M., Oki, R., Oki, T., & Yoshimura, K. (2021). Applicability of a nationwide flood

forecasting system for Typhoon Hagibis 2019. Scientific Reports, 11(1), 10213. https://doi.org/10.1038/s41598-021-89522-8

Moriasi, D. N., Gitau, M. W., Pai, N., & Daggupati, P. (2015). Hydrologic and water quality models: Performance measures and evaluation criteria. Transactions of the ASABE, 58(6), 1763–1785. https://doi.org/10.13031/trans.58.10715

Nihei, Y., Shinohara, A., Ohta, K., Maeno, S., Akoh, R., Akamatsu, Y., Komuro, T., Kataoka, T., Onomura, S., & Kaneko, R. (2019). Flooding along Oda river due to the western Japan heavy rain in 2018. Journal of Disaster Research, 14(6), 874–885. https://doi.org/10.20965/jdr.2019.p0874

Nishimura, S., Takeshita, Y., Nishiyama, S., Suzuki, S., Shibata, T., Shuku, T., Komatsu, M., & Kim, B. (2020). Disaster report of 2018 July heavy rain for geo-structures and slopes in Okayama. Soils and Foundations, 60(1), 300–314. https://doi.org/10.1016/j.sandf.2020.01.009

Nohara, D., Takemon, Y., & Sumi, T. (2020). Real-Time Flood Management and Preparedness: Lessons from Floods Across the Western Japan in 2018. Advances in Hydroinformatics. Springer Water. 287–304. https://doi.org/10.1007/978-981-15-5436-0_22

Shakti, P. C., & Kamimera, H. (2019). Flooding in Oda river basin during torrential rainfall event in July 2018. Engineering Journal, 23(6), 477–485. https://doi.org/10.4186/ej.2019.23.6.477

Shakti, P. C., Kamimera, H., & Misumi, R. (2020). Inundation analysis of the oda river Basin in Japan during the flood event of 6-7 july 2018 utilizing local and global hydrographic data. Water, 12(4). https://doi.org/10.3390/W12041005

Wang, J., Shi, B., Zhao, E., Yuan, Q., & Chen, X. (2022). The long-term spatial and temporal variations of sediment loads and their causes of the Yellow River Basin. Catena, 209. https://doi.org/10.1016/j.catena.2021.105850

Wang, K., Onodera, S., Saito, M., Okuda, N., & Okubo, T. (2021). Estimation of Phosphorus Transport Influenced by Climate Change in a Rice Paddy Catchment Using SWAT. International Journal of Environmental Research, 15(4), 759–772. https://doi.org/10.1007/s41742-021-00350-0

Wang, K., Onodera, S., Saito, M., & Shimizu, Y. (2021). Long-term variations in water balance by increase in percent imperviousness of urban regions. Journal of Hydrology, 602. https://doi.org/10.1016/j.jhydrol.2021.126767

Wang, Y., Shao, J., Su, C., Cui, Y., & Zhang, Q. (2019). The application of improved SWAT model to hydrological cycle study in karst area of south China. Sustainability, 11(18). https://doi.org/10.3390/su11185024

Yoshida, K. (2018). Estimation of Inundation Area and Depth Distribution for the Takahashi River and Hijikawa River Flooding Associated with the Heavy Rain

Event of July 2018. Journal of The Remote Sensing Society of Japan, 38(5), 422–425.

Chapter 4 Analyzing the impacts of influencing factors and slope gradient

4.1 Background and objectives

Sediment yield is a critical environmental concern in many catchments, affecting water quality, reservoir capacity, and aquatic ecosystems. Various factors influence sediment yield, including natural and human-induced factors. The slope is one of the primary factors, where steeper slopes generally lead to higher sediment yields due to increased runoff velocity and erosive power. Additionally, land use practices, soil type, vegetation cover, and rainfall intensity significantly impact sediment yield (X. Liu et al., 2008). For instance, in the Upper Gilo Watershed, the sediment yield varies with the slope gradient, rainfall patterns, and the degree of vegetation cover, emphasizing the need to consider these variables in sediment yield estimation models (Zantet oybitet et al., 2023).

Several management strategies are essential for reducing sediment yield, with best management practices (BMPs) playing a vital role. Practices such as check dams, vegetation planting, and fencing have shown effectiveness in controlling sediment and nutrient yield. Several management practices, like contouring, terracing, grassed waterways, and filter strips, have also been evaluated for their potential benefits. These practices work by reducing runoff velocity, enhancing sediment deposition, and improving water infiltration, thereby minimizing sediment transport to water bodies (X. Liu et al., 2008; Walia et al., 2023).

The impact of slope steepness on sediment yield is extremely significant. Slope gradient significantly influences the velocity and volume of runoff, thus affecting sediment transport and deposition. Studies have shown that steeper slopes tend to have

higher sediment yields due to increased runoff velocity and erosive power. Conversely, gentler slopes promote better water infiltration and sediment deposition (Zhao et al., 2022). Management practices like terracing and contouring are particularly effective on sloped lands as they reduce the slope length and gradient, thereby decreasing runoff speed and enhancing sediment retention (X. Liu et al., 2008; Walia et al., 2023).

Various management practices are commonly applied to catchments to evaluate their sediment trapping capacity for different management practices. SWAT model offers several conservation management operations like terracing, contouring, buffer and filter strips, strip cropping, and grassed waterways. A filter strip, known as a vegetative filter or buffer strip, is a densely vegetated strip placed to intercept runoff and filter the pollutants from upslope areas. Filter strips minimize the amount of pollutants by slowing down overland flow and causing particulates to be deposited (Arnold et al., 2012).

Among the management practices, contour ridges and grass strip practices are the most effective for a gentle slope, while the effectiveness of buffer or filter strips depends on the strip width regardless of the slope (Mtibaa et al., 2018; Nasri, 2007).

This study is conducted to identify and analyze the factors influencing sediment yield and evaluate the slope gradient effect on sediment yield under varying land cover and soil types. Additionally, the study aims to assess the sediment retention capacity of filter strips of different widths and their effectiveness in reducing sediment yield in high-sediment-yield subbasins.

4.2 Materials and method

4.2.1 Identifying influencing factors on sediment yield

We conducted principal component analysis (PCA) on the HRU sediment yield to understand the correlations between different components and identify the factors that influence sediment yield. In PCA, we considered land attribute variables related to soil erosion, including topography, soil, and land use. The components analyzed include CN (daily average curve number), Slope (slope percent rise of HRUs), USLE_K (soil erodibility factor), Sol_AWC (available water capacity of the soil layer), Sol_BD (soil moist bulk density), Sol_K (saturated hydraulic conductivity of soil) and SYLD (sediment yield).

4.2.2 Sediment filter strips scenarios

Filter strips are effective for reducing traditional nonpoint source pollutants. However, several factors must be considered when designing filter strips, such as vegetation characteristics, slope, soil, and strip width (Boger et al., 2018; Zhang et al., 2023). The simulation in this study focused on the filter strip width while the other parameters were kept constant as the SWAT model default. The efficiency of various filter strip widths for retaining sediments in terms of subbasins and the entire catchment is assessed. The calibrated model is used as the baseline scenario. The sediment filter strips are set up in five subbasins with the highest-sediment-yield HRUs of slopes greater than 15%. It is expected that these strips will decrease the sediment output of not only those five individual subbasins but also the entire catchment to a certain extent.

4.3 Results and discussions

4.3.1 Factors influencing high sediment yield

The PCA results (Figure 16) indicated that PC1 and PC2 could explain 44 % and 21% of the variables. PC1 showed strong positive correlations between soil properties and CN but a weak correlation with SYLD. PC2 showed a strong positive correlation between Slope and SYLD, indicating that as the slope increases, the sediment yield increases. PC3 explained the correlations between Sol_AWC and Slope, but this combination showed the weakest correlation with SYLD among all PCs. PC4 showed the second strongest positive correlation between CN and SYLD after PC2. Therefore, Slope and CN influence sediment yield the most.

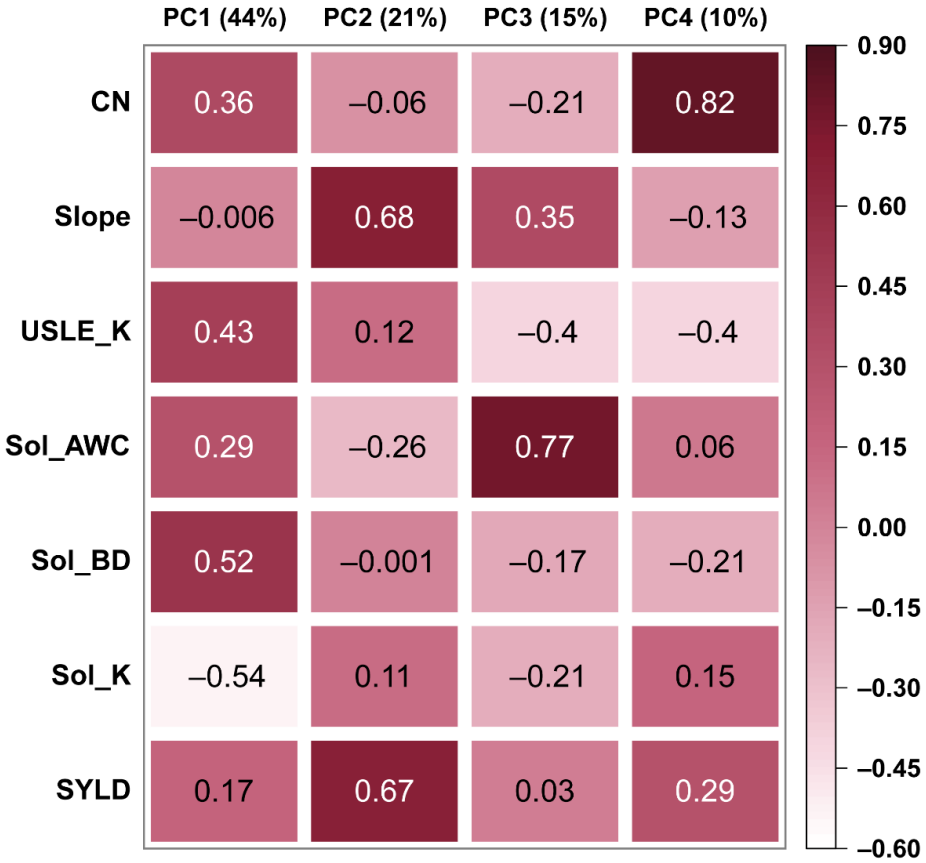

Figure 16 Correlation coefficient of the principal component analysis

According to the PCA results, the sediment yield of the studied catchment is highly influenced by the slope and daily average CN—the main variables that affect surface runoff. In SWAT, the daily average CN is adjusted based on the soil moisture content and land use (Arnold et al., 2012). Several studies have shown that types of land use significantly affect sediment yield (G. Liu et al., 2022; Regasa & Nones, 2023; Sadhwani et al., 2022; Shrestha et al., 2022). However, in this study, the effect of slope sediment yield is higher than that of land use types, making the catchment highly vulnerable to sediment disaster under high precipitation. The factors that control sediment yield vary among catchments, depending on the features of the catchments and their environmental properties. For instance, in eastern US watersheds, due to the low relief of the region, the glacier history and temperature are the most influencing variables for sediment yield, and topography, precipitation, and land use only slightly affect sediment yield (Ahamed, 2014).

4.3.2 Slope gradient effect on sediment yield by different land cover and soil types

The slope gradient effects on sediment yield variations are illustrated in Figure 17, where the average sediment yield of the slope gradients 0%–15%, 15%–30%, 30%–45%, and >45% are 0.15, 0.42, 0.6, and 1.25 ton ha^{-1} yr^{-1}, respectively (Figure 17a). Overall, sediment yields are noticeably higher in the steeper slope classes for all land covers (Figure 17b). Among all the land covers, bare land at a slope of >45% indicated the highest average sediment yield at 2.2 ton ha^{-1} yr^{-1}. Rice, agricultural, and bare land have the highest sediment yield variations against the slope gradient increase. In contrast to bare and agricultural lands, urban areas show the least sediment yield variations against

the slope gradient, which is potentially due to infrastructure that can reduce erosion such as stormwater management systems. Deciduous forests, evergreen forests, and grasslands have comparatively modest sediment yield. Between the major land covers—deciduous and evergreen forests—of the studied catchment, the difference in sediment yield is significant. Evergreen forests have a higher sediment yield than deciduous forests with an increase in slope gradient. However, deciduous forests revealed a notably large range of sediment yield as it becomes steeper with the sediment yield reaching as high as 7.2 tons ha^{-1} yr^{-1}.

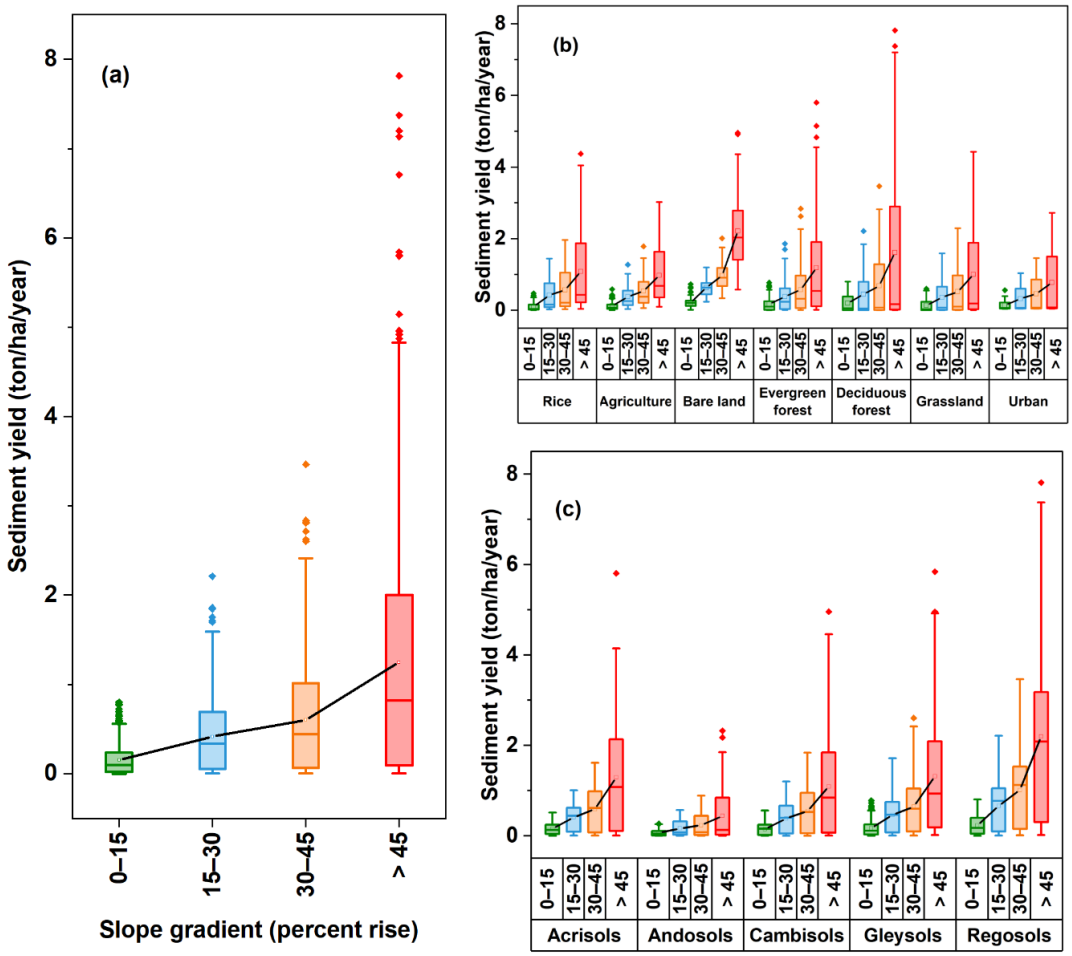

Figure 17 Sediment yield by slope gradient (a) without consideration of different land cover and soil types, (b) at different land cover, (c) at different soil types

The sediment yield variations by slope gradients at different soil types are shown in Figure 17(c). Acrisols, cambisols, and gleysols showed a steady increase in sediment yield with an increasing slope gradient. The sediment yield in andosols increases slowly with increasing slope gradient. Regosols showed a drastic increase in sediment yield with slope steepness with an average sediment yield being 0.23, 0.66, 1, and 2.1 ton ha^{-1} yr^{-1} with slope 0%–15%, 15%–30%, 30%–45%, and >45%, respectively.

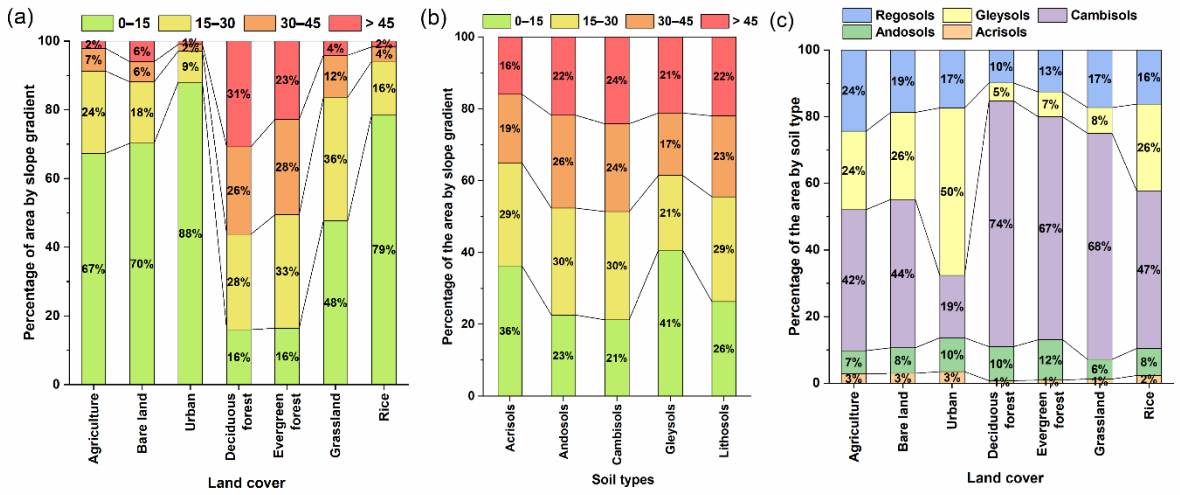

Figure 18 (a) Land cover area percentage distribution per slope gradient, (b) Soil type area percentage distribution per slope gradient, (c) Soil type area percentage for each type of land cover

High sediment yield for the steep slopes of deciduous forests can be influenced, not-withstanding the fact that 31% of this land area type is within the slope gradient of >45%, whereas that of evergreen forests is 23% (Figure 18a). Moreover, deciduous forests showed a broad range in sediment yield with increasing slope (Figure 18b), indicating that for steeper slopes, although most of the deciduous forest has low sediment yield, extreme sediment yield occurs in some parts. Therefore, the deciduous forest steep slope gradient (>45%) in the studied catchment should be prioritized for implementing

soil conservation measures. Besides the slope gradient, the high variation in sediment yield of the deciduous forest could be due to external factors arising from forest management activities. Forest management operations like fewer or no thinning operations result in higher soil loss (Razafindrabe et al., 2010). The forest environmental conditions related to forest management (stand height, species composition and density, root density, litter, and understory vegetation) have a strong influence on sediment yield (Shinohara et al., 2019; Wen et al., 2021). According to Miyata et al. (2009), forest floor coverage can significantly reduce 95% of soil erosion compared to an uncovered forest. The external factors discussed in this section could not be modeled because of the un-availability of detailed data for such a large-scale catchment.

4.3.3 Sediment retention capacity of filter strips

The high-sediment-yield HRUs are mainly located along the river channel of the subbasins 6, 16, 18, 19, and 20 (Figure 14b). Among them, subbasin 16 and 18 are the input subbasins to the Shin-nariwa reservoir. The sediment retention capacity of filter strips with different width for subbasins with high-sediment-yield HRUs is depicted in Figure 19. The results showed that the sediment retention capacity increases as the filter strip becomes wider. The filter strips in subbasins 16 and 18 can reduce the sediment input to the Shin-nariwa reservoir up to 34%. While being adjacent subbasins, 19 and 20 exhibited the same trend for sediment retention; however, subbasin 6 is unique as a 1-m-wide filter strip in that subbasin revealed no substantial reduction in the sediment yield. Nonetheless, the sediment retention capacity in subbasin 6 increased considerably with increasing strip width, starting from 18.5% retention for 2-m-wide strip and eventually realizing 60% retention for 10-m-wide strip. The filter strips in subbasins 19 and 20 are

effective for trapping sediments, exhibiting 34% retention for 1-m-wide strip and reaching 69% for 10-m-wide strip. The results showed that making filter strips, in particular, in the subbasins with the five highest sediment yields can decrease the sediment outputs of the individual subbasins and overall catchment. The filter strips from those specific subbasins can reduce the entire catchment's sediment output from 8.5% to 17.3%. Additionally, a 5-m-wide strip demonstrated the highest efficiency, exhibiting 14% sediment retention in overall catchment sediment output. This is because the sediment retention capacity increase was significant (1% to 2%) when using up to 5-m-wide filter strip and was only marginal (<1%) when using a strip of width >5 m.

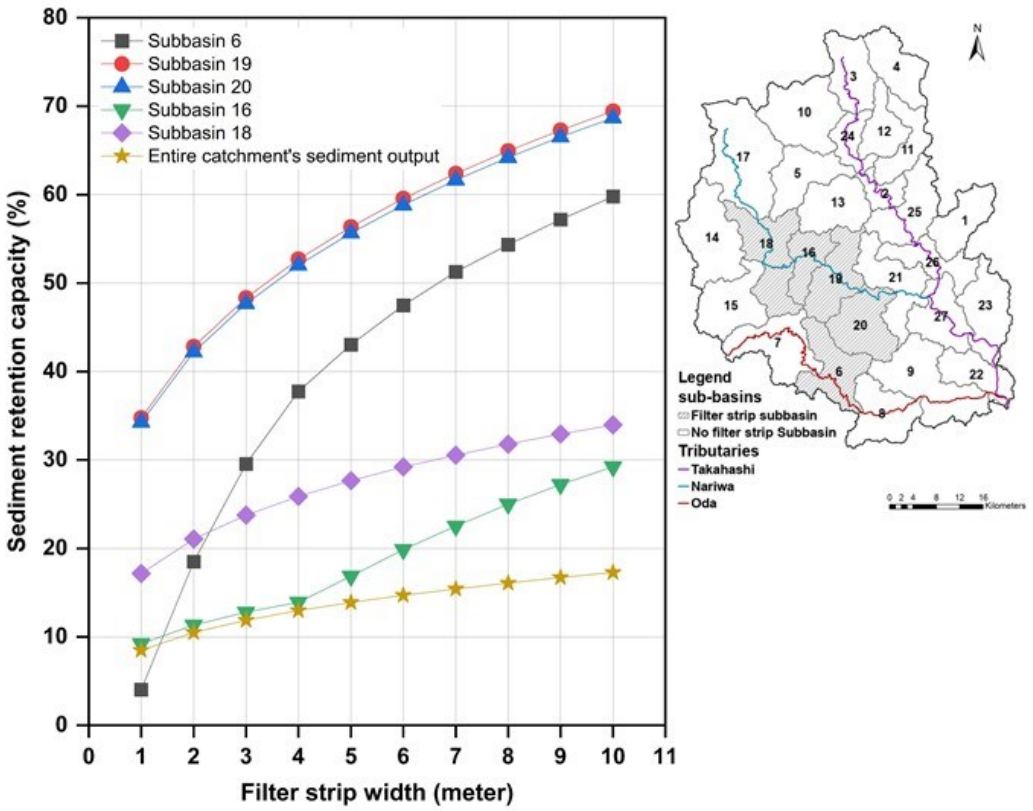

Figure 19 Sediment retention capacity of the filter strips by varying width

The sediment retention capacity exhibited by strips with various widths agreed with the results reported in previous studies by Sirabahenda et al. (2020) and Zhang et al.

(2023). Their results showed that the trapping efficiency flattened after a certain threshold, and once the filter strip width was larger than the threshold limit, the retention capacity increased only marginally with increasing width. The most effective filter strip threshold width in the studied catchment was relatively smaller than that used in the study by Sirabahenda et al, (2020) in the Mill watershed, where a 50-m-wide strip exhibited the most significant retention. Zantet oybitet et al, (2023) found that in the Upper Gilo Watershed, Ethiopia, placing filter strips in the entire catchment could reduce sediments by 34.9% with a 10-m-wide strip and 52% with a 30-m-wide strip. Filter strips with widths of 5, 10, 15, and 20 m could decrease the watershed level sediment to 22%, 25%, 28%, and 30%, respectively, when they were introduced in cropland along the main channel in the Joumine watershed (Mtibaa et al., 2018). Therefore, compared with previous studies, the filter strip practice was more effective in the Takahashi catchment, wherein selective subbasins could hold the sediment by 17.3% with a 10-m-wide strip.

4.4 Conclusions

The study's findings highlighted the important factors influencing sediment yield in Takahashi catchment and the impact of slope gradient by land cover and soil types. Principal Component Analysis (PCA) revealed that slope and daily average curve number (CN) are the primary variables affecting sediment yield. The analysis demonstrated that steeper slopes, especially those above 45%, contribute significantly to higher sediment yields across various land covers, with bare land and agricultural areas showing the most substantial variations.

Specifically, the study found that the average sediment yield increases from 0.15 ton ha^{-1} yr^{-1} for slopes between 0%–15% to 1.25 ton ha^{-1} yr^{-1} for slopes greater than

45%. Among different land covers, bare land exhibited the highest sediment yield at steeper slopes, reaching up to 2.2 ton ha^{-1} yr^{-1}. In contrast, urban areas showed the least variation in sediment yield with slope gradient due to effective infrastructure for erosion control.

The effectiveness of sediment filter strips was also evaluated, indicating that wider strips significantly enhance sediment retention, particularly in high-sediment-yield subbasins. A 10-meter-wide filter strip can reduce sediment yield by up to 69% in certain subbasins. Implementing 5-meter-wide strips was found to be the most efficient, reducing sediment output by 14% across the catchment. The sediment retention capacity increases were significant up to 5 meters in width, beyond which the increase was marginal.

These results provide valuable insights for developing effective sediment management practices and highlight the need for strategies considering the specific characteristics of catchments and their environmental properties. The study underscores the importance of integrating land use planning and slope management in sediment control measures to mitigate the adverse impacts of sediment yield on water bodies and related ecosystems.

4.5 References

Ahamed, A. (2014). Geomorphic and Land Use Controls on Sediment Yield in Eastern USA. http://creativecommons.org/licenses/by/4.0/

Arnold, J. G., Kiniry, J. R., Srinivasan, R., Williams, J. R., Haney, E. B., & Neitsch, S. L. (2012). Input/Output Documentation Soil & Water Assessment Tool.

Boger, A. R., Ahiablame, L., Mosase, E., & Beck, D. (2018). Effectiveness of roadside vegetated filter strips and swales at treating roadway runoff: a tutorial review. Environmental Science: Water Research & Technology, 4(4), 478–486. https://doi.org/10.1039/C7EW00230K

Liu, G., Schmalz, B., Zhang, Q., Qi, S., Zhang, L., & Liu, S. (2022). Assessing effects of land use and land cover changes on hydrological processes and sediment yield in the Xunwu River watershed, Jiangxi Province, China. Frontiers of Earth Science, 16(3), 819–833. https://doi.org/10.1007/s11707-021-0959-9

Liu, X., Zhang, X., & Zhang, M. (2008). Major Factors Influencing the Efficacy of Vegetated Buffers on Sediment Trapping: A Review and Analysis. Journal of Environmental Quality, 37(5), 1667–1674. https://doi.org/10.2134/jeq2007.0437

Miyata, S., Kosugi, K., Gomi, T., & Mizuyama, T. (2009). Effects of forest floor coverage on overland flow and soil erosion on hillslopes in Japanese cypress plantation forests. Water Resources Research, 45(6). https://doi.org/10.1029/2008WR007270

Mtibaa, S., Hotta, N., & Irie, M. (2018). Analysis of the efficacy and cost-effectiveness of best management practices for controlling sediment yield: A case study of the Joumine watershed, Tunisia. Science of The Total Environment, 616–617, 1–16. https://doi.org/10.1016/j.scitotenv.2017.10.290

Nasri, S. (2007). Characteristics and hydrological impacts of a cascade of bench terraces on a semi-arid hillslope in central Tunisia. Hydrological Sciences Journal, 52(6), 1134–1145. https://doi.org/10.1623/hysj.52.6.1134

Razafindrabe, B. H. N., He, B., Inoue, S., Ezaki, T., & Shaw, R. (2010). The role of forest stand density in controlling soil erosion: Implications to sediment-related disasters in Japan. Environmental Monitoring and Assessment, 160(1–4), 337–354. https://doi.org/10.1007/s10661-008-0699-2

Regasa, M. S., & Nones, M. (2023). SWAT model-based quantification of the impact of land use land cover change on sediment yield in the Fincha watershed, Ethiopia. Frontiers in Environmental Science, 11. https://doi.org/10.3389/fenvs.2023.1146346

Sadhwani, K., Eldho, T. I., Jha, M. K., & Karmakar, S. (2022). Effects of Dynamic Land Use/Land Cover Change on Flow and Sediment Yield in a Monsoon-Dominated Tropical Watershed. Water, 14(22), 3666. https://doi.org/10.3390/w14223666

Shinohara, Y., Misumi, Y., Kubota, T., & Nanko, K. (2019). Characteristics of soil erosion in a moso-bamboo forest of western Japan: Comparison with a broadleaved forest and a coniferous forest. Catena, 172, 451–460. https://doi.org/10.1016/j.catena.2018.09.011

Shrestha, S., Binod Bhatta, Talchabhadel, R., & Virdis, S. G. P. (2022). Integrated assessment of the landuse change and climate change impacts on the sediment yield in the Songkhram River Basin, Thailand. Catena, 209, 105859. https://doi.org/10.1016/j.catena.2021.105859

Sirabahenda, Z., St-Hilaire, A., Courtenay, S. C., & van den Heuvel, M. R. (2020). Assessment of the effective width of riparian buffer strips to reduce suspended sediment in an agricultural landscape using ANFIS and SWAT models. Catena, 195, 104762. https://doi.org/10.1016/j.catena.2020.104762

Walia, S., Babbar, R., & Singh, S. (2023). A scenario-based analysis of selected best management practices for reduced sediment and nutrient yield in the watershed located in the Shivalik hills, India. H2Open Journal, 6(3), 463–476. https://doi.org/10.2166/h2oj.2023.033

Wen, Z., Zheng, H., Zhao, H., Liu, L., & Ouyang, Z. (2021). Species compositional, structural and functional diversity exerts different effects on soil erosion caused by increased rainfall intensity in Chinese tropical forests. Plant and Soil, 465(1–2), 97–108. https://doi.org/10.1007/s11104-021-04980-3

Zantet oybitet, M., Sambeto Bibi, T., & Abdulkerim Adem, E. (2023). Evaluation of best management practices to reduce sediment yield in the upper Gilo watershed, Baro akobo basin, Ethiopia using SWAT. Heliyon, 9(10), e20326. https://doi.org/10.1016/j.heliyon.2023.e20326

Zhang, Y., Bhattarai, R., & Muñoz-Carpena, R. (2023). Effectiveness of vegetative filter strips for sediment control from steep construction landscapes. Catena, 226, 107057. https://doi.org/10.1016/j.catena.2023.107057

Zhao, Q., Wang, A., Jing, Y., Zhang, G., Yu, Z., Yu, J., Liu, Y., & Ding, S. (2022). Optimizing Management Practices to Reduce Sediment Connectivity between Forest Roads and Streams in a Mountainous Watershed. Remote Sensing, 14(19), 4897. https://doi.org/10.3390/rs141948

Chapter 5 High-temporal resolution modelling of extreme hydrological events

5.1 Background and objectives

The calibration of a hydrological model can be mainly categorized into two, based on the calibration scheme: time-continuous and event-based calibration. There are several event-based hydrological and sediment yield models. However, those models have the drawbacks that they are data intensive and typically used in small-scale farmland or catchment sediments (Pandey et al., 2016). Among many hydrological models, although the Soil and Water Assessment Tool (SWAT) model is not designed specifically for flood and extreme events, it can capture the events and is used for simulating hydro-climatic extreme conditions in the previous studies (Tan et al., 2020).

Table 5 Hourly suspended sediment simulation studies by SWAT

References	Studied country	Climatic zone	area (km^2)	Process calibrated	Calibration scheme
Kaffas et al. (2018)	Greece	Subtropical	840	streamflow, sediment	Split-site
Meaurio et al. (2021)	Basque country	Temperate	4.6	streamflow, sediment	Event-based
Lee et al. (2024)	South Korea	Temperate	52	streamflow, sediment	Split-site

Numerous studies use the hourly precipitation data input to simulate the daily streamflow and suspended sediment transport. Brighenti et al. (2019) reviewed the 28 hourly SWAT studies and found that majority of the studies used hourly SWAT simulation to simulate the hourly streamflow, however, few studies applied hourly SWAT to suspended sediment simulation as shown in Table 5 (Kaffas et al., 2018; Lee et al., 2024; Meaurio et al., 2021). Additionally, the previous hourly suspended sediment studies were in catchment areas < 1000 km^2, which means the catchment area exhibits less spatial heterogeneity, especially in terms of the precipitation across the catchment.

When planning for the flood mitigation measures and flood risk analysis, it is critical to consider the flood exceedance probability of the studied catchment (Apel et al., 2006; Todini & Reggiani, 2024). The probability of the occurrence of the events based on the historical record data is important when making management and preparedness plans for extreme events (Van Kempen et al., 2021).

The objectives of this study are to assess the accuracy of hourly SWAT modeling in simulating high-flow events for streamflow and sediment with consideration of the exceedance probability in the events selection processes and identify the influence of pre-event antecedent conditions on the model performance.

5.2 Materials and method

Based on the observed data from 2002 – 2007, we selected the events with a daily average flow greater than 500 m^3/s. Therefore, a total of ten extreme events with a flow greater than 500 m^3/s are observed, as listed in Table 6. The annual exceedance of the probability of the events ranged from 15% to 90%, which indicates that the study covers the high-flow events very well. When separating calibration and validation, the events are

well considered based on the exceedance probability so that it will not lead to a bias towards either low or high flow.

Table 6 Selected events for calibration and validation

	Event number	**Event Occurrence**	**highest flow (m^3/s)**	**suspended sediment (mg/l)**	**Annual exceedance probability (%)**
Calibration	I	July 12 to 15, 2003	2235.81	102.7	50
	II	May 15 to 18, 2004	1715.34	116.1	55
	III	Sep 7 to 9, 2004	834.7	127.7	75
	IV	Oct 19 to 23, 2004	3268	188.6	30
	V	June 22 to 27, 2006	1107.54	159.8	70
Validation	VI	Aug 30 to Sep 1, 2004	817.41	192.2	75
	VII	Sep 28 to Oct 1, 2004	2025.95	181	50
	VIII	Sep 4 to 8, 2005	1437.74	129.9	55
	IX	July 16 to 23, 2006	3973.25	125.7	15
	X	July 11 to 18, 2007	1253.12	98.9	60

The selected events can be categorized into three groups depending on the pre-antecedent condition and the precipitation during the events: Group A (moist antecedent condition and low total precipitation events), group B (dry antecedent condition and high total precipitation events), and group C (extreme precipitation pattern with moderate total precipitation events). The events I, II, VII are in group A, the events IV, VIII, IX are in group B, and events II, V, VI are in group C, respectively. Event X is considered an outlier

event where the model performance did not correspond to any other events, which can be either due to some unknown human impacts during the events or observed data quality.

5.3 Results and discussions

5.3.1 Assessment of sub-daily model performance

The calibrated parameters and the calibration ranges are shown in Table 7 and the hourly calibration and validation results of the extreme events are shown in Figure 20. Overall, it is found that the model can simulate the hourly streamflow and suspended sediment satisfactorily. The statistical indexes of the calibrated and validated events are expressed in Table 8. As stated in Tan et al. (2020), there is no standard evaluation criteria for the extreme-based calibration and validation. Therefore, the standard from Moriasi et al. (2015) was used. However, we need to note that the standard criteria in Moriasi et al. (2015) are set for streamflow at daily, monthly, and annual scale and the sediment at monthly scale.

Within the calibration events, events I and III are satisfactorily simulated from the model with the streamflow NSE values of 0.59 and 0.51, and the sediment NSE values of 0.58 and 0.51, respectively (Table 8). Contrarily, events II and V showed unsatisfactory for both streamflow and sediment with the streamflow NSE 0.2 and 0.49, and the sediment NSE 0.42 and 0.21, respectively. Event IV simulated the streamflow satisfactorily with the NSE value 0.69, however, unsatisfactorily for sediment simulation with 0.07.

Table 7 Calibrated parameters for hourly high-flow events' streamflow and sediment

	Modification type	Parameter Name	Description	Minimum	Maximum	Fitted	Remark
Flow	r	CN2	SCS runoff curve number	-0.1	0.1	-0.018	FRSD
						-0.009	FRSE
				0	0.25	0.13	URBN
						0.14	BARR
						0.15	AGRL
						0.07	RICE
						0.13	GRAS
	v	RCHRG_DP	Deep aquifer percolation fraction	0.2	0.35	0.33	
	v	ESCO	Soil evaporation compensation factor	0.2	0.8	0.31	
	r	SOL_K	Saturated hydraulic conductivity	-0.15	0.15	0.017	
	r	SOL_AWC	Available water capacity of the soil layer	-0.2	0.2	0.05	
	r	SOL_BD	Moist bulk density	-0.1	0.1	0.01	
	v	GWQMN	Threshold depth of water in the shallow aquifer required for the return flow to occur (mm)	100	1500	418	
	v	CH_N2	Manning's "n" value for the main channel	0.04	0.1	0.059	
	r	HRU_SLP	Average slope steepness	-0.25	0	-0.1	
	v	ALPHA_BF	Baseflow alpha factor (days)	0.5	1	0.71	
	v	MSK_CO1	Calibration coefficient for normal flow	0.03	0.15	0.13	
	v	MSK_CO2	Calibration coefficient for low flow	0.04	0.15	0.12	

	Modification type	Parameter Name	Description	Minimum	Maximum	Fitted	Remark
	v	MSK_X	Weighing factor for inflow and outflow	0.05	0.3	0.3	
	v	CNCOEF	Plant ET curve number coefficient	1	2	1.98	
	v	GW_REVAP	Groundwater "revap" coefficient	0.02	0.08	0.027	
Sediment	v	CH_COV1	Channel erodibility factor	0.01	0.4	0.24	
	v	CH_COV2	Channel cover factor	0.01	0.2	0.069	
	v	C_FACTOR	Cover and management factor for overland flow erosion	0.002	0.012	0.006	
	v	ADJ_PKR	Peak rate adjustment factor for sediment routing	0.5	1.5	1.11	
	v	EROS_SPL	Splash erosion coefficient	0.9	2	1.17	
	v	RILL_MULT	Rill erosion coefficient	0.5	0.75	0.71	
	v	CH_D50	Median particle diameter of main channel (mm)	10	60	11.25	
	v	OV_N	Manning's n overland flow	0.5	2	1.8	

Note: r indicates that the parameter value is changed relatively, and v indicates that the default parameter is replaced

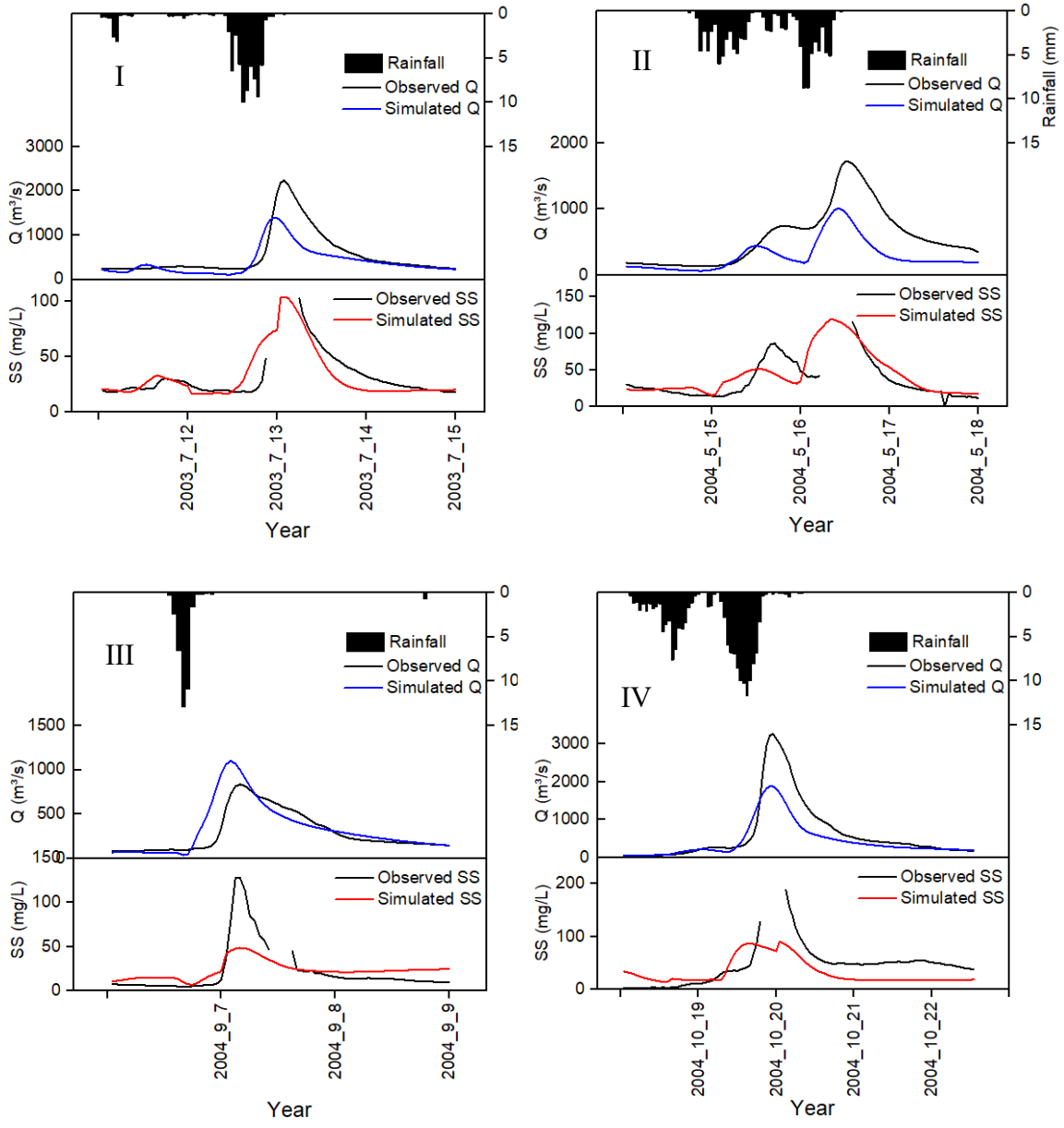
I
Rainfall
Observed Q
Simulated Q
Q (m³/s)
Observed SS
Simulated SS
SS (mg/L)
2003_7_12
2003_7_13
2003_7_14
2003_7_15
Year
II
Rainfall (mm)
2004_5_15
2004_5_16
2004_5_17
2004_5_18
III
2004_9_7
2004_9_8
2004_9_9
IV
2004_10_19
2004_10_20
2004_10_21
2004_10_22

(cont'd)

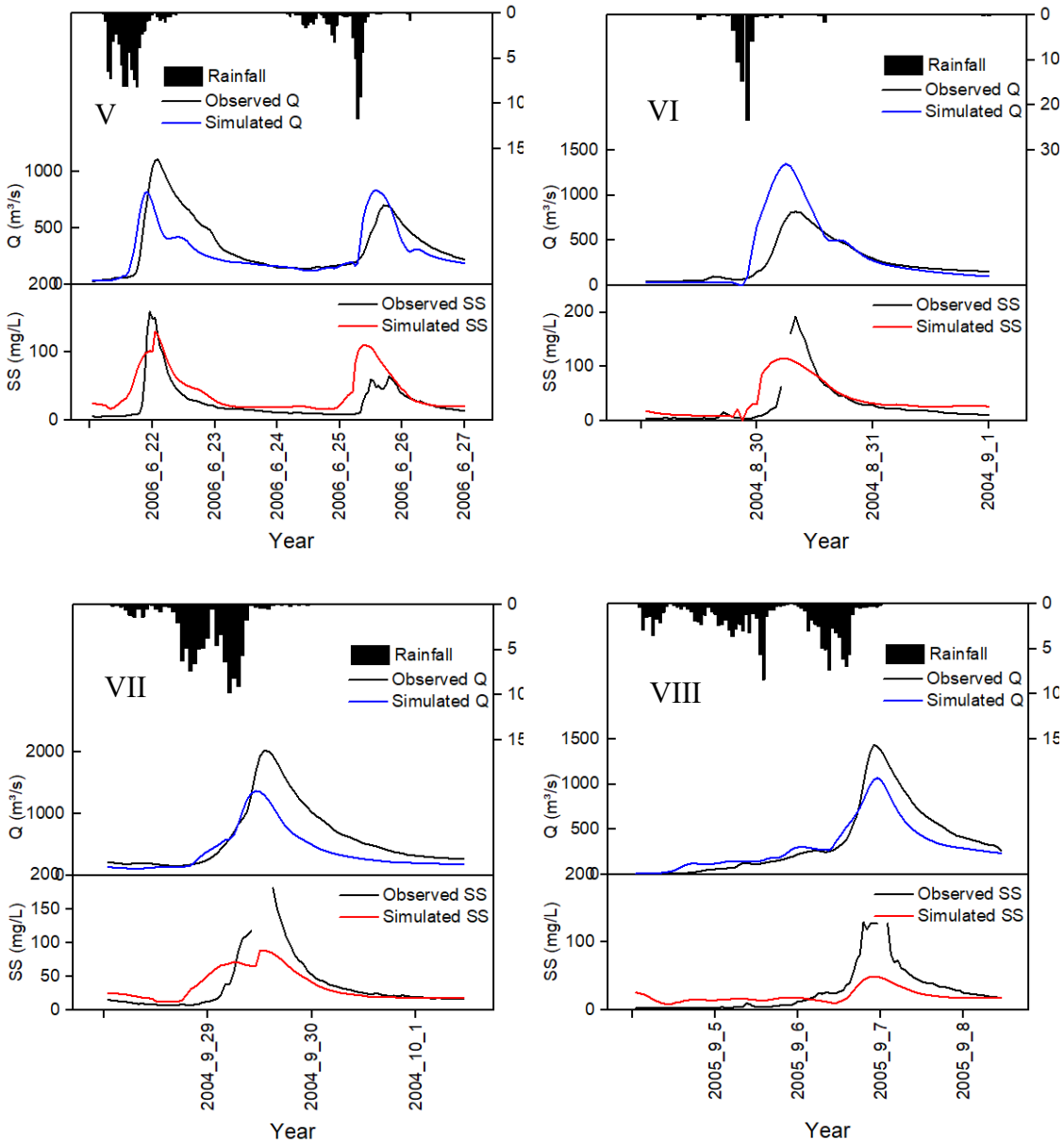
V
Rainfall
Observed Q
Simulated Q
Q (m³/s)
Observed SS
Simulated SS
SS (mg/L)
2006_6_22
2006_6_23
2006_6_24
2006_6_25
2006_6_26
2006_6_27
Year
VI
2004_8_30
2004_8_31
2004_9_1
VII
2004_9_29
2004_9_30
2004_10_1
VIII
2005_9_5
2005_9_6
2005_9_7
2005_9_8

(cont'd)

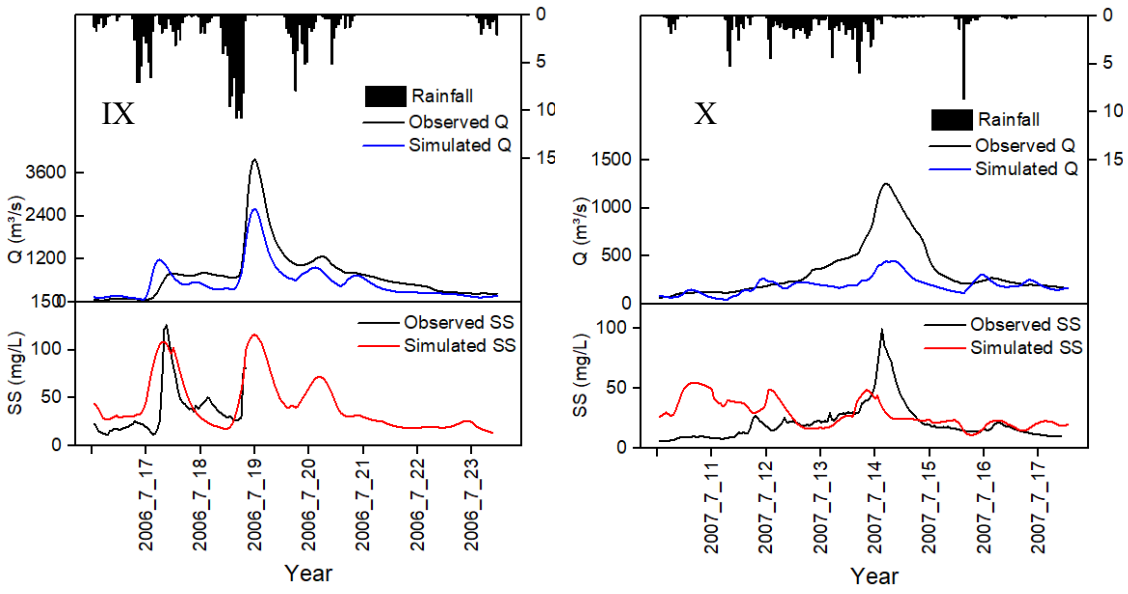

Figure 20 Observed and simulated hourly calibration and validation events

Table 8 Statistical performance of the hourly model

Event		Streamflow		Sediment	
		NSE	PBIAS	NSE	PBIAS
Calibration	I	**0.59**	26.7	**0.58**	**6.45**
	II	0.2	49.23	0.42	**-10.34**
	III	**0.51**	**-13.88**	**0.51**	**-2.76**
	IV	**0.69**	30.58	0.07	34.81
	V	0.49	16.53	0.21	-54.94
Validation	VI	-0.09	**8.49**	**0.54**	-27.55
	VII	**0.59**	34.14	**0.57**	**4.54**
	VIII	**0.83**	**14.34**	0.41	24.54
	IX	**0.71**	27.99	-0.05	-29.1
	X	0.15	42.88	-0.69	-33.9

Within the validation events, events VII and VIII are satisfactory for both streamflow and sediment, where it performed the NSE streamflow 0.59 and 0.83, and the sediment 0.63 and 0.83, respectively. Event X is the only event with both unsatisfactory streamflow and sediment simulation. Event VI is unsatisfactory for streamflow with -0.09, however, satisfactory for sediment with 0.54. Reversely, the model simulation for event IX is satisfactory for streamflow with NSE 0.71 whereas unsatisfactory for sediment with -0.05.

5.3.2 Simulation of historical extreme events

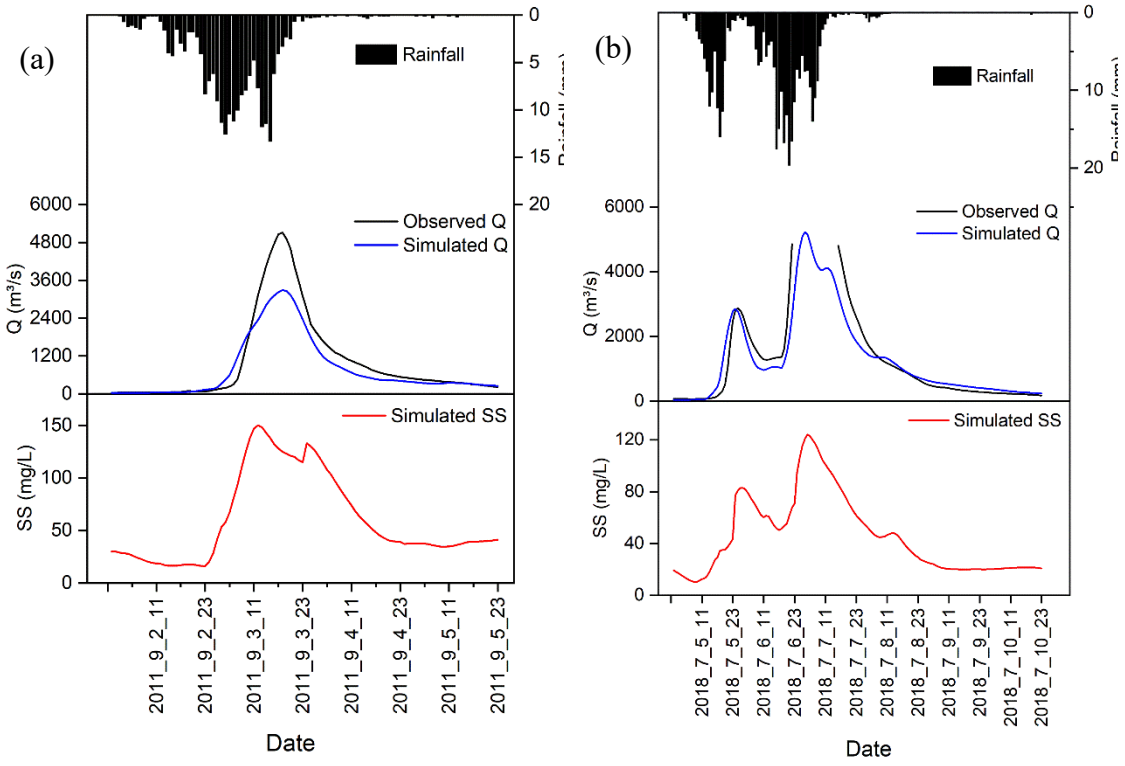

Figure 21 Simulated streamflow and suspended sediment during the high-flow events occurred in (a) 2011, (b) 2018

The studied area experienced two significant high-flow events according to the observed streamflow data: one in 2011 with the observed streamflow of 5,112 m³/s and

the other event in 2018 with the highest observable streamflow of 4,852 m^3/s. For 2018, the streamflow mentioned here is only the highest observable streamflow as there was high flow and flooding during the event, and the gauging station was out of functioning. The NSE and PBIAS values for 2011 events were 0.85 and 23, whereas NSE and PBIAS values for 2018 were 0.82 and 8.7, respectively, for the streamflow. The model simulated the maximum suspended sediment concentration of 2011 as 150 mg/L and 2018 as 124 mg/L (Figure 21).

5.3.3 Relationship of pre-event antecedent conditions and the model performance

The hourly model simulation is satisfactory for group A in both streamflow and sediment (Figure 22). In group B, it showed that streamflow simulation is satisfactory but unsatisfactory for the sediment. The events for group C act reversely between streamflow and sediment. Although the values are unsatisfactory, if the performance in streamflow is acceptable, the performance in the sediment is unacceptable, like event V, and vice versa in events II and VI. Therefore, in streamflow simulation, the hourly model in SWAT provides satisfactory performance on the events with moist antecedent conditions and low total precipitation events and the events with dry antecedent conditions and high total precipitation events. However, the model performance for sediment simulation is satisfactory for the moist antecedent conditions and low total precipitation events.

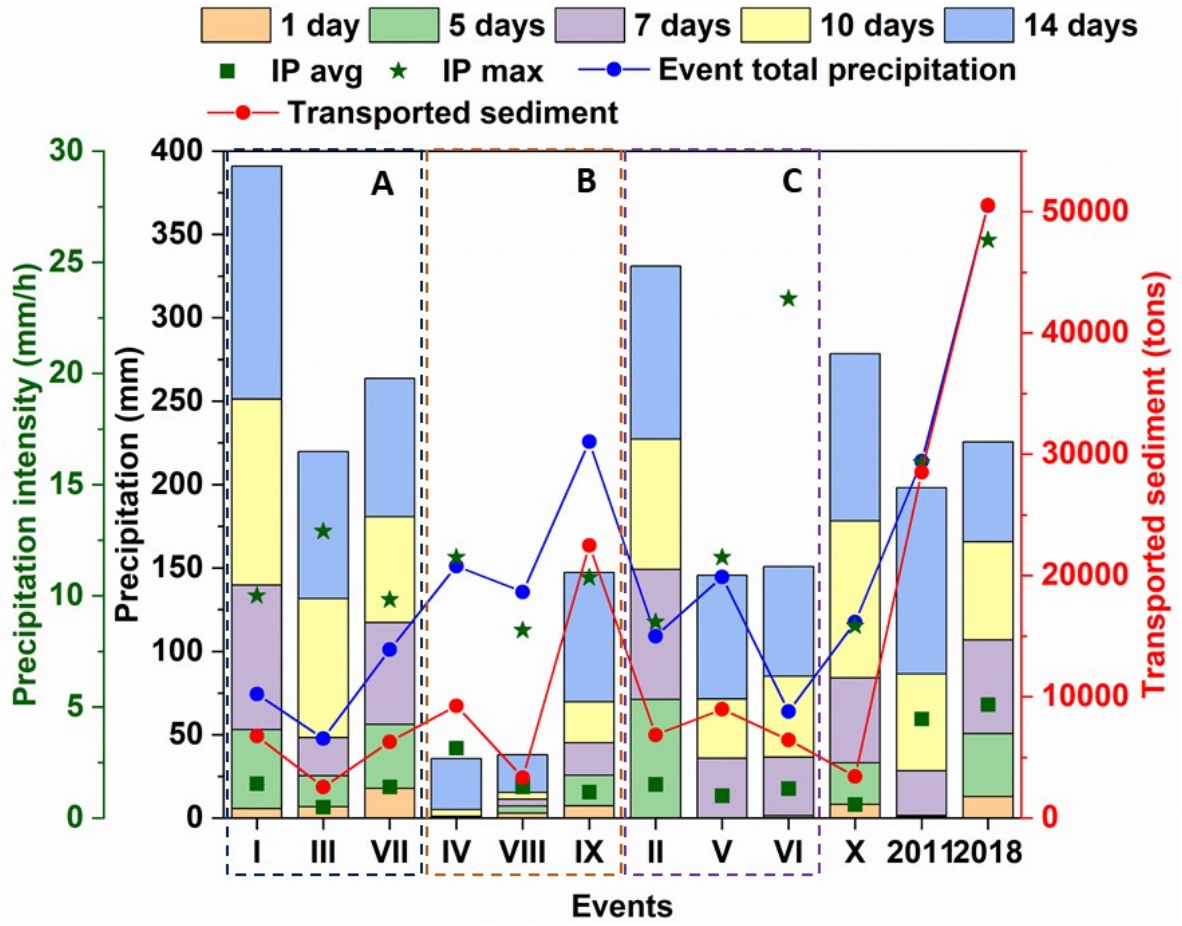

Figure 22 Pre-antecedent conditions of the events, the total precipitation, the precipitation intensity during the events and the transported sediment during the events (IP avg: Average precipitation intensity during the event, IP max: Maximum precipitation intensity during the event)

According to Figure 22, the sediment transported during the events is influenced by both the total precipitation and the precipitation intensity. Generally, the sediment followed the trend of the total precipitation. However, there are some exceptional events. Event VI has lower total precipitation than event VIII but has higher sediment transport than event VIII. The results showed the influence of the precipitation intensity during the event as the maximum precipitation intensity of event VI is much higher than event VIII.

The total precipitation and precipitation effects can be clearly visible in the 2018 event, with the highest sediment transported among all the other events. Although the suspended sediment concentration simulated in 2018 is lower than in 2011, the total sediment transported is high due to the longer event period, and there were two peaks, as shown in Figure 21. The results are consistent with the findings of Wang et al. (2018), where higher runoff and sediment yield occurred in high-intensity rainfall compared to low and moderate rainfall intensities

5.3.4 The influence of the precipitation spatial variations on the events transported sediment

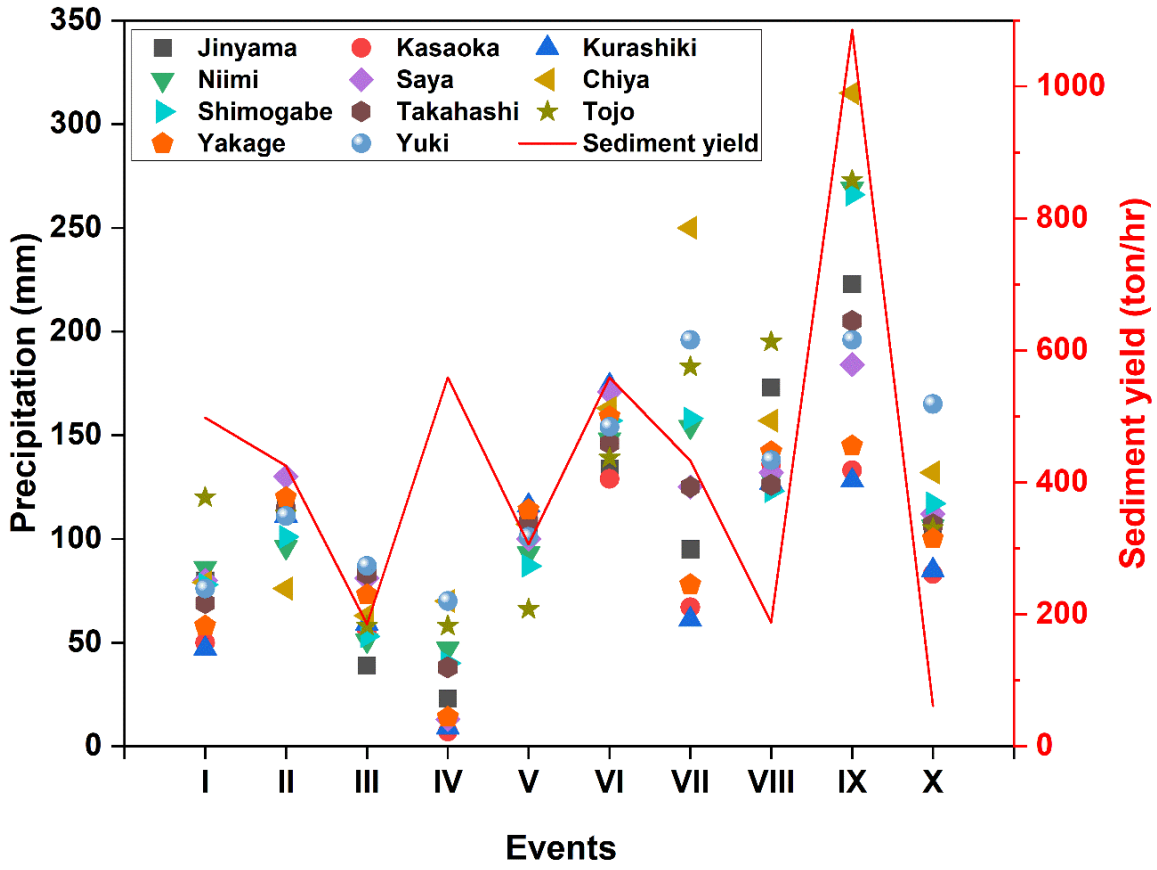

Figure 23 Total precipitation observed in each meteorological station and the sediment yield

As the studied catchment has high spatial heterogeneity in precipitation, the total precipitation during each event by stations and the sediment yield during the events are illustrated in Figure 23, to assess the influence of precipitation spatial variations on the sediment yield. It was found that Tojo and Saya stations have strong influence on the sediment transport in the Takahashi catchment. The sediment yield was high when the total precipitation in Tojo or Saya station was relatively high as in events I, II, IV, VI, and IX, whereas the sediment yield is low when the total precipitation of Tojo or Saya station is low as in the events III, and V. This can be related to the fact that Tojo and Saya stations are in the high sediment yield subbasins of Takahashi catchment based on the sediment yield spatial variations results from Figure 14(a).

5.4 Conclusions

This study evaluated the performance of the SWAT model for simulating extreme hydrological events at a high temporal resolution within the Takahashi catchment. The model performance varied significantly depending on the pre-antecedent moisture conditions and precipitation patterns of the event.

The sub-daily model showed satisfactory performance for events with moist antecedent conditions and low total precipitation (Group A) and events with dry antecedent conditions and high total precipitation (Group B). However, for events with extreme precipitation patterns and moderate total precipitation (Group C), the model performance was less consistent, often showing a trade-off between satisfactory simulation of streamflow and sediment.

The calibrated sub-daily model was applied to simulate historical extreme events in 2011 and 2018. It showed that the 2018 events transported the highest sediment load

amongst all the events simulated in this study. Analysis revealed that sediment transport was not substantially proportional to total precipitation. Although the sediment transported during the events generally followed the trend of total precipitation, it is found that the precipitation intensity highly influences the sediment transport in some events. Due to high spatial variations in precipitation across the catchment, stations like Tojo and Saya significantly influenced sediment yield, indicating that localized heavy precipitation in high sediment yield subbasins could drive sediment transport more than overall precipitation amounts.

In conclusion, while the SWAT model demonstrates potential for simulating extreme hydrological events at a high temporal resolution, its performance depends on the specific characteristics of each event. Moreover, the importance of the spatial variations of precipitation is highly noticeable in modeling extreme events in large catchments.

5.5 References

Apel, H., Thieken, A. H., Merz, B., & Blöschl, G. (2006). A Probabilistic Modelling System for Assessing Flood Risks. Natural Hazards, 38(1–2), 79–100. https://doi.org/10.1007/s11069-005-8603-7

Brighenti, T. M., Bonumá, N. B., Srinivasan, R., & Chaffe, P. L. B. (2019). Simulating sub-daily hydrological process with SWAT: a review. Hydrological Sciences Journal, 64(12), 1415–1423. https://doi.org/10.1080/02626667.2019.1642477

Kaffas, K., Hrissanthou, V., & Sevastas, S. (2018). Modeling hydromorphological processes in a mountainous basin using a composite mathematical model and ArcSWAT. Catena, 162, 108–129. https://doi.org/10.1016/j.catena.2017.11.017

Lee, S., Lim, K. J., & Kim, J. (2024). Analysis of Effects of Spatial Distributed Soil Properties and Soil Moisture Behavior on Hourly Streamflow Estimate through the Integration of SWAT and LSM. Sustainability, 16(4). https://doi.org/10.3390/su16041691

Meaurio, M., Zabaleta, A., Srinivasan, R., Sauvage, S., Sánchez-Pérez, J. M., Lechuga-Crespo, J. L., & Antiguedad, I. (2021). Long-term and event-scale sub-daily

streamflow and sediment simulation in a small forested catchment. Hydrological Sciences Journal, 66(5), 862–873. https://doi.org/10.1080/02626667.2021.1883620

Moriasi, D. N., Gitau, M. W., Pai, N., & Daggupati, P. (2015). Hydrologic and water quality models: Performance measures and evaluation criteria. Transactions of the ASABE, 58(6), 1763–1785. https://doi.org/10.13031/trans.58.10715

Pandey, A., Himanshu, S. K., Mishra, S. K., & Singh, V. P. (2016). Physically based soil erosion and sediment yield models revisited. In Catena (Vol. 147, pp. 595–620). https://doi.org/10.1016/j.catena.2016.08.002

Tan, M. L., Gassman, P. W., Yang, X., & Haywood, J. (2020). A review of SWAT applications, performance and future needs for simulation of hydro-climatic extremes. Advances in Water Resources (Vol. 143). https://doi.org/10.1016/j.advwatres.2020.103662

Todini, E., & Reggiani, P. (2024). Toward a New Flood Assessment Paradigm: From Exceedance Probabilities to the Expected Maximum Floods and Damages. Water Resources Research, 60(1). https://doi.org/10.1029/2023WR034477

Van Kempen, G., Van Der Wiel, K., & Anna Melsen, L. (2021). The impact of hydrological model structure on the simulation of extreme runoff events. Natural Hazards and Earth System Sciences, 21(3), 961–976. https://doi.org/10.5194/nhess-21-961-2021

Wang, Y., You, W., Fan, J., Jin, M., Wei, X., & Wang, Q. (2018). Effects of subsequent rainfall events with different intensities on runoff and erosion in a coarse soil. Catena, 170, 100–107. https://doi.org/10.1016/j.catena.2018.06.

Chapter 6 Discussion and conclusion

6.1 Effects of rock types on the hydrological and sediment yield in the studied catchment

As geological information was not considered during model setup, the SWAT model may be inaccurate when simulating groundwater systems. This is significant in modeling limestone-dominated catchments with complicated surface and groundwater interactions as limestone circulates water similarly to surface streams in normal conditions and functions similarly to confined flow conditions under flood conditions (Baffaut & Benson, 2009; Sear et al., 1999). There have been several methods used in the SWAT modeling of groundwater-dominated catchments. Some studies combined field investigations with SWAT to simulate limestone-dominated watersheds. For instance, Jakada and Chen (2020) used the tracer test and Senent-Aparicio et al. (2020) used the chloride mass balance method together with SWAT for limestone watersheds. Other studies modified the linear reservoir module in groundwater flow in the SWAT into multiple reservoir modules for modeling the interbasin groundwater flows in karstic areas. For example, Nerantzaki et al. (2015), Nguyen et al. (2020), and Nikolaidis et al. (2013) applied a modified two-reservoir module and Wang et al. (2019) used a modified three-reservoir module, considering a nonlinear relationship between groundwater recharge and discharge.

The SWAT model satisfactorily simulated the Takahashi catchment with 5.3% of limestone area. The calibration strategy practiced in this study was similar to one of the calibration schemes used in Sánchez-Gómez et al. (2022), where the GWQMN parameter was calibrated specially for the high-groundwater-contribution regions formed by

carbonated rocks. In the studied catchment, field observations revealed that the Takahashi tributary is a catchment with karst groundwater flow. Groundwater flow from the limestone directly contributes to the Takahashi tributary (Figure 7). Similar to the Takahashi tributary, the Nariwa tributary has a low GWQMN value, and thus, high groundwater flow. However, the high groundwater flow in the Nariwa tributary is attributed to the effects of limestone or the very steep slope.

The geologically complex Takahashi catchment's sediment yield is higher than the Hii River and Ishikari River in Japan, which are reported to be 0.27 tons ha^{-1} yr^{-1} and 0.11 tons ha^{-1} yr^{-1}, respectively (Duan et al., 2015; Somura et al., 2012). Lithology and geomorphology significantly impact sediment output (de Vente et al., 2011; Li et al., 2019; Shi et al., 2014; Wang et al., 2015; Zhang et al., 2022). The effects of rock types on the sediment yield in the Takahashi catchment were reported. Therein, sandstone-dominated subbasins tended to have high sediment yields, such as subbasins 6, 14, 20, and 21. The sandstone found in high-sediment-yield subbasins was tertiary sandstone, which was not resistant to erosion. According to the landslide warning areas issued by MLIT, slope failures and landslides were dominant in these subbasins. Meanwhile, the granite and limestone-dominant subbasins of the Takahashi catchment showed low sediment yields. These findings agree with previous studies. For instance, Gomi et al. (2005) showed that sandstone-dominated catchments have higher sediment yields than other geologies. Meanwhile, rhyolitic rocks are extremely resistant to erosion, whereas granites have the lowest sediment yield potentials (Clapp et al., 2002; Karki & Shibano, 2007; Ono et al., 2011). Li et al. (2019) reported that the carbonate rocks in karstic regions have less runoff and consequently have low sediment yields. The chalk stream catchment

shows lower sediment yields than the others even though the major land use was by agriculture (Heywood & Walling, 2003).

6.2 Sediment yield influencing factor variations in catchments under climate change

Catchment sediment yield is influenced by a variety of factors, and these can be significantly altered under the impacts of climate change. One of the main factors under climate change is the precipitation patterns. Changes in the intensity, frequency, and duration of rainfall events can lead to increased erosion and sediment transport (Gonzalez-Hidalgo et al., 2012). More intense rainfall can result in greater runoff, which in turn can increase the soil detachment and transportation from the upland area to the river system (Sun et al., 2021).

Temperature changes also play an important role in sediment yield variations. The increase in temperature can accelerate the soil erosion rate by affecting soil moisture content, vegetation cover, and soil structure (Poesen et al., 2003). Higher temperatures can increase the evapotranspiration rates, reduce the soil moisture and making soils more susceptible to erosion (Lal, 2001). Additionally, temperature changes can impact the type and distribution of vegetation, which is the protection to the ground cover (García-Ruiz et al., 2015).

The changes in the precipitation and temperature can also alter the river flow regimes, which can contribute to variations in sediment yield (Milly et al., 2005). Changes in flow regimes can affect the sediment transport capacity of rivers, with potential increases in flood frequencies leading to higher sediment yields during storm events (Walling & Fang, 2003). Additionally, temperature increase can change the snowmelt patterns, resulting in alteration of the timing and magnitude of river flows, thereby

affecting sediment transport processes (Barnett et al., 2005). In addition to the natural climate change phenomenon, human interventions aimed at adapting to climate change, such as the construction of dams and reservoirs, can also significantly modify sediment yield in catchments, by altering the sediment trapping and releasing timing and magnitude (Syvitski et al., 2005; Vörösmarty et al., 2003).

6.3 Direction for future studies

According to Figure 9, we can see that some of the high-flow events are underestimated by the mode, especially in the sediment yield. Seasonal calibration can reduce the uncertainties in the hydrological model in simulating the streamflow (Cibin et al., 2010; Fu et al., 2015). In this study, seasonal calibration may improve the streamflow simulations. However, if we look at the simulated hydrograph, we can see that most high-flow events with the observed high sediment load are not always associated with high streamflow (especially the events in 2003 and 2004). In those events, although the streamflow was not high, the sediment concentration was high, which led to the high sediment load. This can be caused by other processes that the current model cannot consider in the simulation, such as debris flows and landslides. Chiang et al. (2021) and Lu & Chiang, (2019) studies stated that SWAT-TWN, a modified version of SWAT integrated with landslide simulation for sediment, provides better simulation than the standard SWAT in Taiwan. The landslide mechanisms differ significantly from place to place due to various factors such as geological formations, climate, topography, land use, and human activities (Crosta & Frattini, 2008; Cruden & Varnes, 1996; Dai et al., 2002; Glade et al., 2005). Therefore, in the future, integrating the compatible debris flow and landslides algorithm into the SWAT model may improve the model simulation, particularly for steep and heavy precipitation catchments like the studied catchment.

The studied catchment exhibits significant spatial variation in precipitation. According to Chordia et al. (2022), the impact of precipitation on streamflow simulation is more pronounced in areas with steep slopes compared to the influences of topography and land cover. Additionally, the steep slopes significantly influence the sediment yield in the catchment. Therefore, utilizing finer spatial resolution precipitation input data, along with high-resolution topography, may help reduce model uncertainties.

6.4 References

Barnett, T. P., Adam, J. C., & Lettenmaier, D. P. (2005). Potential impacts of a warming climate on water availability in snow-dominated regions. Nature, 438(7066), 303–309. https://doi.org/10.1038/nature04141

Chiang, L.-C., Liao, C.-J., Lu, C.-M., & Wang, Y.-C. (2021). Applicability of modified SWAT model (SWAT-Twn) on simulation of watershed sediment yields under different land use/cover scenarios in Taiwan. Environmental Monitoring and Assessment, 193(8), 520. https://doi.org/10.1007/s10661-021-09283-9

Chordia, J., Panikkar, U. R., Srivastav, R., & Shaik, R. U. (2022). Uncertainties in Prediction of Streamflows Using SWAT Model—Role of Remote Sensing and Precipitation Sources. Remote Sensing, 14(21), 5385. https://doi.org/10.3390/rs14215385

Cibin, R., Sudheer, K. P., & Chaubey, I. (2010). Sensitivity and identifiability of stream flow generation parameters of the SWAT model. Hydrological Processes, 24(9), 1133–1148. https://doi.org/10.1002/hyp.7568

Claire Baffaut, & Verel W Benson. (2009). Modeling Flow and Pollutant Transport in a Karst Watershed with SWAT. Transactions of the ASABE, 52(2), 469–479. https://doi.org/10.13031/2013.26840

Clapp, E. M., Bierman, P. R., & Caffee, M. (2002). Using 10Be and 26Al to determine sediment generation rates and identify sediment source areas in an arid region drainage basin. Geomorphology, 45(1–2), 89–104. https://doi.org/10.1016/S0169-555X(01)00191-X

Crosta, G. B., & Frattini, P. (2008). Rainfall-induced landslides and debris flows. Hydrological Processes, 22(4), 473–477. https://doi.org/10.1002/hyp.6885

Cruden, D. M., & Varnes, D. J. (1996). Landslide types and processes, Special report, Transportation research board, National Academy of Sciences, 247:36-75

Dai, F. C., Lee, C. F., & Ngai, Y. Y. (2002). Landslide risk assessment and management: an overview. Engineering Geology, 64(1), 65–87. https://doi.org/10.1016/S0013-7952(01)00093-X

de Vente, J., Verduyn, R., Verstraeten, G., Vanmaercke, M., & Poesen, J. (2011). Factors controlling sediment yield at the catchment scale in NW Mediterranean geoecosystems. Journal of Soils and Sediments, 11(4), 690–707. https://doi.org/10.1007/s11368-011-0346-3

Duan, W. L., He, B., Takara, K., Luo, P. P., Nover, D., & Hu, M. C. (2015). Modeling suspended sediment sources and transport in the Ishikari River basin, Japan, using SPARROW. Hydrology and Earth System Sciences, 19(3), 1293–1306. https://doi.org/10.5194/hess-19-1293-2015

Fu, C., James, A. L., & Yao, H. (2015). Investigations of uncertainty in SWAT hydrologic simulations: a case study of a Canadian Shield catchment. Hydrological Processes, 29(18), 4000–4017. https://doi.org/10.1002/hyp.10477

García-Ruiz, J. M., Beguería, S., Nadal-Romero, E., González-Hidalgo, J. C., Lana-Renault, N., & Sanjuán, Y. (2015). A meta-analysis of soil erosion rates across the world. Geomorphology, 239, 160–173. https://doi.org/10.1016/j.geomorph.2015.03.008

Glade, T., Anderson, M., & Crozier, M. J. (Eds.). (2005). Landslide Hazard and Risk. Wiley. https://doi.org/10.1002/9780470012659

Gomi, T., Moore, R. D., & Hassan, M. A. (2005). Suspended sediment dynamics in small forest streams of the Pacific Northwest. Journal of the American Water Resources Association, 41(4), 877–898. https://doi.org/10.1111/j.1752-1688.2005.tb03775.x

Gonzalez-Hidalgo, J. C., Batalla, R. J., Cerda, A., & de Luis, M. (2012). A regional analysis of the effects of largest events on soil erosion. Catena, 95, 85–90. https://doi.org/10.1016/j.catena.2012.03.006

Heywood, M. J. T., & Walling, D. E. (2003). Suspended sediment fluxes in chalk streams in the Hampshire Avon catchment, U.K. Hydrobiologia (Vol. 494).

Jakada, H., & Chen, Z. (2020). An approach to runoff modelling in small karst watersheds using the SWAT model. Arabian Journal of Geosciences, 13(8). https://doi.org/10.1007/s12517-020-05291-0

Karki, K. B., & Shibano, H. (2007). Sediment yield and transportation capacity in a forested watershed underlain by weathered granite. 59(5), 35–42.

Lal, R. (2001). Soil degradation by erosion. Land Degradation & Development, 12(6), 519–539. https://doi.org/10.1002/ldr.472

Li, Z., Xu, X., Zhu, J., Xu, C., & Wang, K. (2019). Effects of lithology and geomorphology on sediment yield in karst mountainous catchments. Geomorphology, 343, 119–128. https://doi.org/10.1016/j.geomorph.2019.07.001

Lu, C.-M., & Chiang, L.-C. (2019). Assessment of Sediment Transport Functions with the Modified SWAT-Twn Model for a Taiwanese Small Mountainous Watershed. Water, 11(9), 1749. https://doi.org/10.3390/w11091749

Milly, P. C. D., Dunne, K. A., & Vecchia, A. V. (2005). Global pattern of trends in streamflow and water availability in a changing climate. Nature, 438(7066), 347–350. https://doi.org/10.1038/nature04312

Nerantzaki, S. D., Giannakis, G. V., Efstathiou, D., Nikolaidis, N. P., Sibetheros, I. A., Karatzas, G. P., & Zacharias, I. (2015). Modeling suspended sediment transport and assessing the impacts of climate change in a karstic Mediterranean watershed. Science of the Total Environment, 538, 288–297. https://doi.org/10.1016/j.scitotenv.2015.07.092

Nguyen, V. T., Dietrich, J., & Uniyal, B. (2020). Modeling interbasin groundwater flow in karst areas: Model development, application, and calibration strategy. Environmental Modelling and Software, 124. https://doi.org/10.1016/j.envsoft.2019.104606

Nikolaidis, N. P., Bouraoui, F., & Bidoglio, G. (2013). Hydrologic and geochemical modeling of a karstic Mediterranean watershed. Journal of Hydrology, 477, 129–138. https://doi.org/10.1016/j.jhydrol.2012.11.018

Ono, K., Akimoto, T., Gunawardhana, L. N., Kazama, S., & Kawagoe, S. (2011). Distributed specific sediment yield estimations in Japan attributed to extreme-rainfall-induced slope failures under a changing climate. Hydrology and Earth System Sciences, 15(1), 197–207. https://doi.org/10.5194/hess-15-197-2011

Poesen, J., Nachtergaele, J., Verstraeten, G., & Valentin, C. (2003). Gully erosion and environmental change: importance and research needs. Catena, 50(2–4), 91–133. https://doi.org/10.1016/S0341-8162(02)00143-1

Sánchez-Gómez, A., Martínez-Pérez, S., Pérez-Chavero, F. M., & Molina-Navarro, E. (2022). Optimization of a SWAT model by incorporating geological information through calibration strategies. Optimization and Engineering, 23(4), 2203–2233. https://doi.org/10.1007/s11081-022-09744-1

Sear, D. A., Armitage, P. D., & Dawson, F. H. (1999). Groundwater dominated rivers. Hydrological Processes, 13(3), 255–276. https://doi.org/10.1002/(SICI)1099-1085(19990228)13:3<255::AID-HYP737>3.0.CO;2-Y

Senent-Aparicio, J., Alcalá, F. J., Liu, S., & Jimeno-Sáez, P. (2020). Coupling SWAT model and CMB method for modeling of high-permeability bedrock basins

receiving interbasin groundwater flow. Water, 12(3). https://doi.org/10.3390/w12030657

Shi, Z. H., Huang, X. D., Ai, L., Fang, N. F., & Wu, G. L. (2014). Quantitative analysis of factors controlling sediment yield in mountainous watersheds. Geomorphology, 226, 193–201. https://doi.org/10.1016/j.geomorph.2014.08.012

Somura, H., Takeda, I., Arnold, J. G., Mori, Y., Jeong, J., Kannan, N., & Hoffman, D. (2012). Impact of suspended sediment and nutrient loading from land uses against water quality in the Hii River basin, Japan. Journal of Hydrology, 450–451, 25–35. https://doi.org/10.1016/j.jhydrol.2012.05.032

Sun, L., Zhou, J. L., Cai, Q., Liu, S., & Xiao, J. (2021). Comparing surface erosion processes in four soils from the Loess Plateau under extreme rainfall events. International Soil and Water Conservation Research, 9(4), 520–531. https://doi.org/10.1016/j.iswcr.2021.06.008

Syvitski, J. P. M., Vörösmarty, C. J., Kettner, A. J., & Green, P. (2005). Impact of Humans on the Flux of Terrestrial Sediment to the Global Coastal Ocean. Science, 308(5720), 376–380. https://doi.org/10.1126/science.1109454

Vörösmarty, C. J., Meybeck, M., Fekete, B., Sharma, K., Green, P., & Syvitski, J. P. M. (2003). Anthropogenic sediment retention: major global impact from registered river impoundments. Global and Planetary Change, 39(1–2), 169–190. https://doi.org/10.1016/S0921-8181(03)00023-7

Walling, D. E., & Fang, D. (2003). Recent trends in the suspended sediment loads of the world's rivers. Global and Planetary Change, 39(1–2), 111–126. https://doi.org/10.1016/S0921-8181(03)00020-1

Wang, Y., Shao, J., Su, C., Cui, Y., & Zhang, Q. (2019). The application of improved SWAT model to hydrological cycle study in karst area of south China. Sustainability, 11(18). https://doi.org/10.3390/su11185024

Wang, Z.-Y., Lee, J. H. W., & Melching, C. S. (2015). River Dynamics and Integrated River Management. Springer. https://doi.org/10.1007/978-3-642-25652-3

Zhang, F., Zeng, C., Wang, G., Wang, L., & Shi, X. (2022). Runoff and sediment yield in relation to precipitation, temperature and glaciers on the Tibetan Plateau. International Soil and Water Conservation Research, 10(2), 197–207. https://doi.org/10.1016/j.iswcr.2021.09.004

Publication during the Doctoral course

Nang, Y.W.; Onodera, S.-i.; Wang, K.; Shimizu, Y.; Saito, M. Slope Gradient Effects on Sediment Yield of Different Land Cover and Soil Types. Water 2024, 16, 1419. https://doi.org/10.3390/w16101419